

Reply to Reviewer 1

Specific comments: Methods – Line 113: IUPAC has done away with ‘equivalents’, alkalinities are now reported in moles.

We thank the reviewer for catching this. It is now in $\mu\text{mol kg}^{-1}$.

Lines 116, 128, 212: The Millero (2010) constants are not particularly dependable. Perhaps better to use the constants of Cai and Wang (1998). See: Orr, J. C., Epitalon, J. M., and Gattuso, J. P. (2015). Comparison of ten packages that compute ocean carbonate chemistry. *Biogeosciences* 12(5), 1483–1510.

We thank the reviewer for point out the interesting discussion about K_1 and K_2 of Millero (2010) in Orr et al. (2015). Using the constants of Cai and Wang (1998) leads to calculated DIC that ranged from being 0.23% lower, to 0.09% higher than those calculated from Millero (2010), with an average of 0.09% lower. That is, the difference is pretty insignificant. Nevertheless, we have chosen to use Cai and Wang (1998) to calculate DIC.

Lines 127-128: Was TALK corrected for silicate and phosphate contributions? What about the contributions of organic alkalinity? The latter can be very significant in the case of estuaries draining marshes and organic-rich soils, often accounting for the circum-neutral or even acidic nature of these waters. Uncorrected TALK values, combined with pCO_2 measurements, would generate erroneous DIC values. The authors note that DOC makes up about 20% of the DIC, it surely has a large (negative) contribution to Talk.

TALK was not corrected for silicate and phosphate. As we state in Lines 127-130: “The measured TALK and pCO_2 from SharkTREx 2 were used to calculate DIC using CO2SYS (Pierrot et al., 2006) and the dissociation constants of (Millero, 2010), and the results were $1.3 \pm 1.1\%$ (range: -2.4 to +4.4%) higher than the measured DIC, possibly indicating a slight contribution (ca. 1%) to TALK from organic or particulate material, as the samples were not filtered.”

The fact that the calculated DIC agree well with the measured DIC means that the contribution from organic alkalinity was minimal (ca. 1%), assuming that the dissociations constants used to calculate DIC are correct.

Lines 135-136: How were the DOC measurements calibrated and what was their reproducibility and accuracy?

The TOC analyzer was standardized using 10 and 50 ppm of potassium hydrogen phthalate (KHP), with reagent water as a blank. The analytical precision based on replicates of KHP is ca. ± 0.3 ppm. We have added this information to the manuscript.

Lines 144-145: What was the reproducibility of the $\delta^{13}\text{C}$ measurements?

Reproducibility was 0.2 ‰ as determined by repeated analysis of internal DIC standards.

We have added this information to the manuscript.

Line 154: What were the $\delta^{13}\text{C}$ standards?

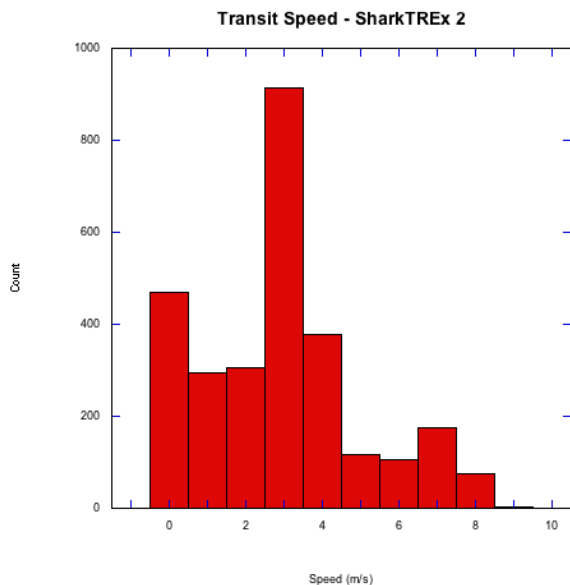
In order to measure the different isotopic ranges within the collected samples, an isotopic calibration was based on two external standards of potassium hydrogen phthalate (KHP - 29.8‰, OI-Analytical) and glutamine (-11.45‰, Fisher) with a concentration range of 0–25 ppm. These standards were prepared in synthetic seawater to match the sample matrix's salinity. The isotope values of these two standards were determined by using an elemental analyzer isotope ratio mass spectrometer (EA-IRMS). We have added this information to the manuscript

Lines 158-159: What was the time constant of the probe? These probes have a slow response and do not provide real-time measurements. The quality of the measurements will depend on the cruising speed of the boat or current velocity. Hence, these measurements may carry a spatial (and temporal) uncertainty.

See next response.

Line 160: The time constant of the optode is even larger than the galvanic sensor. Although the optode response does not drift as much as the galvanic sensor, the precision of the optode is significantly worse than the galvanic sensor. What is the uncertainty on these two measurement methods?

The stated response time of the galvanic sensor is <10 s to reach 90% of final value, and <16 s to reach 95% of final value. As the reviewer states, the time constant of the optode is longer than the galvanic sensor. It has a stated response time of <25 s to reach 63% of final value. The boat speed during the experiments was typically ca. 3 m/s (ca. 6 knots) (see figure below). The other measurements such as the underway SF_6 and pCO_2 measurements also have their associated delay between when the water is taken into the SF_6 extraction system or pCO_2 equilibrator and then the gases finally reach the GC/ECD or NDIR analyzer for analysis. This delay is built-in to the LABVIEW program that assigns GPS position information to the individual measurements based on tests done on the delay in the laboratory. If the delayed response were not corrected, this would lead to a typical offset in location of ca. 50-100 m (less than 1% of the length of the river). Furthermore, most of the measurements are referenced to salinity instead of GPS position, making the exact position less important. Finally, the calculated difference between the effects of conservative mixing and estuarine input on DO in this manuscript were based on relative differences in oxygen, so accuracy of the DO measurements will not significantly affect the results.



Lines 163-164: Even if the authors refer the reader to detailed descriptions in other papers, they should briefly describe the method and its uncertainties.

We have added brief descriptions of the underway SF₆ system.

Lines 200, 206: Are the gas transfer velocities scaled for wind velocity or turbulence generated by flow in the shallow estuary? The authors should provide the estimated value of the gas transfer velocity in the study setting.

The gas transfer velocities are affected by both wind and currents, and we have added that to the manuscript. On Lines 191-193, we stated: “ $k(600)$ for SharkTREx 1 and 2, determined from the parameterization proposed in Ho et al. (2016), were 3.5 ± 1.0 and 4.2 ± 1.8 cm h⁻¹, respectively.” The details for gas exchange in Shark River is given in Ho, D. T., N. Coffineau, B. Hickman, N. Chow, T. Koffman, and P. Schlosser (2016), Influence of current velocity and wind speed on air-water gas exchange in a mangrove estuary, *Geophys. Res. Lett.*, 43, doi:10.1002/2016GL068727.

Lines 219-220: The seawater that intrudes at these shallow depths is likely to be supersaturated with respect to calcite and aragonite, but could become undersaturated by accumulating metabolic CO₂ generated by microbial degradation of dissolved or particulate organic matter in the sediment/karst.

Agreed. We now specify this in the text:

In the manuscript (lines 219-220), we wrote: "Groundwater in this region is likely to contain DIC from CaCO₃ dissolution that occurs when saltwater intrudes into the karst aquifer that underlies this region (Price et al., 2006)." We expanded on this with: "Groundwater in this region is likely to contain DIC from CaCO₃ dissolution that occurs when saltwater intrudes into the karst aquifer that underlies this region (Price et al., 2006), as well as DIC from sediment organic matter mineralization."

Line 234: As noted above, dissolution in saline groundwaters can only occur upon the addition metabolic CO₂ to the groundwaters from microbial degradation of organic matter. Hence, how would the authors distinguish this contribution of 13C-depleted DIC from that of the mangrove-derived organic matter?

We assumed that all organic matter added in the estuary is from the mangroves.

Line 256: Again, what about the metabolic DIC contribution from groundwaters? Mn and Fe oxide reduction will also generate alkalinity.

The DIC from groundwater is assumed to be either from calcite dissolution or from microbial degradation of organic matter. As we specify in the text, the calculation of [DIC]_{dissolution} from [TAlk]_{estuary} provides an upper-bound estimate of the contribution of dissolution to DIC as it does not take into account the contribution of other mineralization pathways to total alkalinity.

In mangrove sediments, aerobic respiration and sulfate reduction are generally the main organic matter degradation pathways, and in our case this is supported by Figure 6, which shows that the contributions of Fe and Mn reduction are likely small.

Also, Fe concentrations in Shark Slough sediments are very low (1.1 mg gdw⁻¹; Chambers, R. M., and Pederson, K. A.: Variation in soil phosphorus, sulfur, and iron pools among south Florida wetlands, *Hydrobiologia*, 569, 63-70, 10.1007/s10750-006-0122-3, 2006), and Mn is expected to be similarly low in this carbonate/mangrove peat setting.

Furthermore, the agreement between measured and calculated DIC (discussed above) indicates that in this environment, the other sources of alkalinity are small, compared to carbonate alkalinity.

Line 265, Eqn. (9), 270-271: What about groundwater contributions?

Groundwater added in the estuary is part of [DOC]_{estuary}

Results and Discussion - Lines 311-312: Somewhat repetitive. Any statistics on this correlation?

We have removed this repetitive statement.

Line 326: Very large and surely contributes to the titration alkalinity.

See reply above regarding measured DIC vs. DIC calculated from TAlk and pCO₂.

Lines 366-368: I noted this earlier. Why not include it in the mass balance equations?

Because that is either considered to be calcite dissolution or microbial degradation of mangrove organic matter.

Line 371: Under what conditions would this occur? Any evidence that aragonite and high Mg-calcites are being dissolved and replaced by low Mg-calcite?

Since we do not know whether isotopic exchange happens during dissolution and re-precipitation, we have removed this paragraph.

Lines 375, 382: Where and under what conditions is CaCO_3 being dissolved? In organic-rich sediments, anaerobic respiration leads to alkalinity production (as indicated earlier), and likely a flux of alkalinity and DIC to the overlying waters. The fluxes would be modulated by neutralization of alkalinity as it diffuses through the oxic sediment layer and by CaCO_3 precipitation in the anoxic sediments.

Dissolution/re-precipitation of CaCO_3 is omnipresent in Florida, but this was not one of the processes examined during SharkTREx 1 and 2. Previous studies (e.g., Stalker et al, 2009) have shown that, surface waters in Florida show higher Sr/Ca ratio than expected from seawater. Even though Sr/Ca released by dissolution is the same as seawater because aragonite Sr/Ca is the same as seawater Sr/Ca, re-precipitation of calcite rejects Sr, which elevates the Sr/Ca ratio.

Stalker, J. C., R. M. Price, and P. K. Swart: Determining Spatial and Temporal Inputs of Freshwater, Including Submarine Groundwater Discharge, to a Subtropical Estuary Using Geochemical Tracers, Biscayne Bay, South Florida, *Estuar Coast*, 32, 694-708, doi:10.1007/s12237-009-9155-y, 2009.

Line 384: See previous comment. This is speculative in the absence of evidence that this dissolution-precipitation process is active.

We agree, and have removed this speculative sentence.

Lines 386-388: The authors need to show how these estimates were derived as sulfate reduction does not appear in the mass balance equations.

The ratio of TALK to DIC for calcite dissolution is 2, and that of sulfate reduction and aerobic respiration are 0.99 and -0.2, respectively. Hence, to achieve the observed ratios of TALK to DIC of 0.84, 0.92, and 0.90 for the three cases, and given the contribution of calcite dissolution of 30%, the contribution of sulfate reduction and aerobic respiration could be calculated using straightforward algebra (assuming no contribution from Fe and Mn reduction). We have stated this more explicitly in the manuscript.

Lines 394-396: The oxidation of these metabolites does not follow the same stoichiometry as aerobic oxidation of organic matter. In the case of H_2S , the redox reaction requires the exchange of 8 electrons (S(-II) to S(+VI)), 2 in the case on Mn^{2+} (to Mn(+IV)) and one for Fe^{2+} (to Fe(+III)).

Here, we meant O_2 to CO_2 stoichiometry. Oxygen uptake due to the re-oxidation of reduced metabolites from sulfate, iron, and manganese reduction results in carbon to oxygen stoichiometry that is similar to aerobic respiration. For that reason, the uptake of

oxygen is equivalent to total carbon mineralization if there is complete re-oxidation of metabolites and denitrification is negligible (see Canfield, 1993; Hulth et al. 1999; Reimers et al., 1992). Therefore, the estimate can be considered as a lower-bound estimate of total carbon mineralization.

Canfield, D. E.: Organic Matter Oxidation in Marine Sediments, in: Interactions of C, N, P and S Biogeochemical Cycles and Global Change, edited by: Wollast, R., Mackenzie, F. T., and Chou, L., Springer Berlin Heidelberg, Berlin, Heidelberg, 333-363, 1993.

Hulth, S., Aller, R. C., and Gilbert, F.: Coupled anoxic nitrification/manganese reduction in marine sediments, *Geochim. Cosmochim. Acta*, 63, 49-66, 10.1016/S0016-7037(98)00285-3, 1999.

Reimers, C. E., Jahnke, R. A., and McCorkle, D. C.: Carbon fluxes and burial rates over the continental slope and rise off central California with implications for the global carbon cycle, *Glob. Biogeochem. Cycle*, 6, 199-224, 10.1029/92GB00105, 1992.

Lines 405:-406: This statement makes little sense, unless the preferential degradation of ^{13}C -enriched OM took place before respiration in the mangrove forest.

We thank the reviewer for catching this, and have revised the statement. This statement was a remnant from an early draft. Initial $\delta^{13}\text{C}_{\text{DOC}}$ data did include salinity correction following the method detailed in Ya et al. (2015), where the standards were match to the salinity range of the samples with synthetic seawater mixtures, with a maxim salinity varying from 30 to 32 depending on the timing and reported salinities of the sampling period. In the revised $\delta^{13}\text{C}_{\text{DOC}}$ data, the lowest observed values from SharkTREx 1 was $-31.6 \pm 1.25 \text{‰}$, as shown in Figure 4d. Previous studies of DOC from mangrove-dominated systems have reported values as low as -30.4‰ (Dittmar, et al, 2006), and some of the more depleted samples from SharkTREx 1 might have DOC sourced from algae associated with mangrove roots, which can have relatively depleted values (Kieckbush et al, 2004).

Dittmar, T. , Hertkorn, N. , Kattner, G. and Lara, R. J.: Mangroves, a major source of dissolved organic carbon to the oceans , *Global Biogeochemical Cycles*, 20, GB1012. doi: 10.1029/2005GB002570, 2006.

Kieckbusch, D.K., Koch, M.S., Serafy, J.E., and Anderson, W.T.: Trophic linkages of primary producers and consumers in fringing mangroves of tropical lagoons, *Bulletin of Marine Science*, v. 74, no. 2, p. 271-285, 2004.

Ya, C., Anderson, W., and Jaffé, R.: Assessing dissolved organic matter dynamics and source strengths in a subtropical estuary: Application of stable carbon isotopes and optical properties, *Continental Shelf Research*, 92, 98-107, 10.1016/j.csr.2014.10.005, 2015.

Reply to Reviewer 2

Major comments

The technique by which the authors quantify gas fluxes is clear and robust, though error estimates would be helpful. It's the longitudinal fluxes, as the authors call them, that cause confusion. As the authors use the term, the longitudinal flux is averaged over the time period of the tracer release and hence accounts for tidal dispersion as well as the net downstream advective transport. The problem is that the authors use the term too broadly and in ways that defy notions of mass conservation. I specifically take issue with a longitudinal flux due to a certain source, such as freshwater wetlands, mangroves, calcium carbonate, or the ocean (lines 18-21); or due to a certain process, such as estuarine or non-estuarine (lines 289-290 and Table 4), and respiration or dissolution (lines 217-218). A longitudinal flux is due to movement of water and nothing else. It's a term in the mass conservation equation that is separate from internal sources and sinks. The two should not be mixed up.

It is true that longitudinal water flux would be due solely to movement of water. However, longitudinal carbon flux is due to movement of water and the concentration of dissolved carbon in the water. When we talk about contributions, we are not talking about the contribution of the freshwater marsh, mangroves, or carbonate to the water movement, but to the dissolved carbon concentration.

We have clarified this in the revised manuscript. For example, we have changed this sentence in the abstract:

“Approximately 80% of the total dissolved carbon flux from all sources (i.e., freshwater wetlands, mangrove, carbonate dissolution, and marine input) out of the Shark and Harney Rivers during these experiments was as inorganic carbon, either via air-water CO₂ exchange or longitudinal flux of inorganic carbon to the coastal ocean.”

To:

“Approximately 80% of the total dissolved carbon flux out of the Shark and Harney Rivers during these experiments was in the form of inorganic carbon, either via air-water CO₂ exchange or longitudinal flux of dissolved inorganic carbon (DIC) to the coastal ocean..”

In the methods section, we have changed:

“As with the inventory calculations, longitudinal fluxes were separated into estuarine and non-estuarine contributions.”

To:

“In addition, using the estuarine and non-estuarine fractions of the inventories in equation (12) allowed the estuarine and non-estuarine proportions of the longitudinal carbon fluxes to be quantified.”

Also confusing is the alternation between approaches based on inventories and approaches based

on fluxes. My suggestion is to focus on a budget approach because this paper is basically about the carbon balance of two estuaries. The final budget is shown in a key figure towards the end of the paper (Figure 5), which clearly shows the control volume approach I am recommending. Remarkably, there is not a single budget equation in the paper. And the method for determining the freshwater wetlands flux shown in this figure should be detailed in the methods, not the figure caption. In the paper, the authors should start with a budget equation and then use inventory equations, such as Equations 2 and 9, as needed to support the budget approach. Budget equations should be shown for DOC, DIC, oxygen, and (perhaps) alkalinity.

We recognize that what the reviewer is suggesting is one valid approach, but we have taken what we feel is an equally valid approach. Determining the carbon balance in the estuaries was not our main goal, although in determining the main sources and sinks, we do eventually arrive there.

Our goal is to determine the export (fluxes to the coastal ocean and across the air-water interface) of mangrove derived carbon from the estuary. We took the approach: Flux = Inventory/Residence Time, where residence times were determined from the tracer release experiments. Hence, in order to determine mangrove derived DIC and DOC fluxes, we needed to find out how much DIC and DOC were in the rivers (i.e., the inventory), and also the sources of this carbon (mangrove vs. calcite dissolution). Then, we needed to determine the fate of the mangrove-derived carbon in the river (i.e., lost to the atmosphere vs. lost to the coastal ocean).

We are not alternating between an inventory and flux approach. We are systematically using the inventory to determine the flux.

A process that appears to be missing in the paper is organic mineralization inside the estuary. The very low DO suggests quite significant net heterotrophy. The authors lump organic mineralization inside the estuary with mangrove root respiration and call it a mangrove source of DIC. Those seem like two very different sources to me, which could perhaps be distinguished using the isotopes. Figure 5 is remarkable in that it does not show any in situ production or consumption. The net organic matter remineralization should be revealed in the DO budget of the individual terms. The “Evidence from DO” section (3.3.3) should basically detail the DO budget: gas exchange, upstream input, downstream export, net in situ consumption, etc. And this budget could be nicely shown in an additional panel on Figure 5.

We consider all organic matter added in the estuary as mangrove derived, so the reviewer is correct that we consider DIC produced from organic mineralization inside the estuary as mangrove derived carbon. In the final budget, it does not matter whether the mineralization occurred in the mangrove sediments, or in the river.

Photosynthesis in the river is ignored, which may be reasonable, but the authors need to be more convincing (lines 228-231). Saying chlorophyll is low is not enough. They state that diurnal pCO₂ variations are small but provide no data to support that. Please be quantitative.

As we state in the manuscript, photosynthesis in the river is ignored because of low chl *a* and low phytoplankton biomass. With respect to day/night pCO₂ variations, we make continuous hourly measurements of pCO₂ from Shark River. The average difference in pCO₂ during the night (6p to 5:59a local time) is 3% lower than during the day (6a to 5:59p local time), a small

amount and not in the direction one might expect if photosynthesis were significant. We have added this quantification to the manuscript.

The choice of endmembers is not clear. How exactly are these chosen and what are the values?

We write in the manuscript that “the freshwater and marine end-members were assigned to the values measured at the lowest (Tarpon Bay) and highest salinities, respectively.” Basically, we went as far as up river and out to the Gulf of Mexico as we could with the boat that we had, and we chose those measurements as the end-members. As we state in the paper, “During SharkTREx 1, the salinity along the longitudinal transects ranged from 1.2 to 27.1, and the mean (\pm s.d.) water temperature was 23.4 ± 0.2 °C. During SharkTREx 2, salinity ranged from 0.6 to 27.1, and water temperatures averaged 22.7 ± 0.9 °C.”

The use of $X \pm Y$ throughout the text (lines 192, 299, 319, 333, 343, 375, etc.) and tables (1, 2, and 3) is unclear. How are X and Y computed? Am I supposed to take Y as a standard deviation or a standard error? What is the sample size for computing X and Y.

Depending on the parameter, the error estimates are based on standard deviations of the measured parameters, or the propagated errors of variables used to calculate the parameter.

Some of the values that the reviewer questioned are quoted from other published papers (e.g., line 192), whereas we do specify that we are quoting the mean and standard deviation in others (e.g., line 299):

“During SharkTREx 1, the salinity along the longitudinal transects ranged from 1.2 to 27.1, and the mean (\pm s.d.) water temperature was 23.4 ± 0.2 °C. During SharkTREx 2, salinity ranged from 0.6 to 27.1, and water temperatures averaged 22.7 ± 0.9 °C.”

We have indicated the number of samples used to calculate mean \pm s.d. in the appropriate places in the manuscript, and have specified in the caption to the tables how \pm are calculated.

Minor comments

Line 25: I think the area referred to here in this flux is the forest area, but the authors should make it clear to remove any ambiguity.

Yes, we have added language that indicates that flux is from the forest.

Line 26: To be clear that you are not talking about the Everglades in general, I would replace “in this region” with “for the Shark and Harney Rivers”

Done

I was pleased to see that the authors recognize the likelihood of large seasonality in the carbon cycle of south Florida estuaries (Section 3.7). However, the authors give no indication as to why they chose to sample in November two years in a row instead of sampling once in the wet season and once in the dry season, which would have given them a sense of the importance of

seasonality. All I am asking for here is a few sentences in the intro or methods describing the rationale for the sampling periods chosen.

There was no good scientific reason for choosing to conduct the experiments in November, twice. SharkTREx 1 and 2 were piggy-backed on funded experiments that took the team from Hawaii to Florida, and these funded experiments had to be conducted in November. SharkTREx 1 was a pilot experiment, and focused on just the Shark River, had fewer stations, and where some important measurements were not made (e.g., DIC). SharkTREx 2 was a follow up to fill some of the gaps (i.e., more stations, Harney River, and high quality DIC measurements). Future studies will be conducted in the dry season.

Dissolved carbon biogeochemistry and export in mangrove-dominated rivers of the Florida Everglades

David T. Ho¹, Sara Ferrón¹, Victor C. Engel^{2,3}, William T. Anderson^{4,5}, Peter K. Swart⁶, René M. Price^{4,5}, Leticia Barbero⁷

5 ¹Department of Oceanography, University of Hawaii, Honolulu, Hawaii 96822, USA

²South Florida Natural Resources Center, Everglades National Park, Homestead, Florida 33030, USA

³Now at: U.S. Forest Service, Fort Collins, Colorado 80526, USA

⁴Southeast Environmental Research Center, Florida International University, Miami, Florida 33199, USA

⁵Department of Earth and Environment, Florida International University, Miami, Florida 33199, USA

10 ⁶Marine Geosciences, Rosenstiel School of Marine and Atmospheric Science, University of Miami, Miami, Florida 33149, USA

⁷NOAA Atlantic Oceanographic and Meteorological Laboratory, Miami, Florida 33149, USA

Correspondence to: David T. Ho (david.ho@hawaii.edu)

15 **Abstract.** The Shark and Harney Rivers, located on the southwest coast of Florida, USA, originate in the freshwater, karstic marshes of the Everglades and flow through the largest contiguous mangrove forest in North America. In November 2010 and 2011, dissolved carbon source-sink dynamics were examined in these rivers during SF₆ tracer release experiments. Approximately 80% of the total dissolved carbon flux put of the Shark and Harney Rivers during these experiments was in the form of inorganic carbon, either via air-water CO₂ exchange or longitudinal flux of
20 dissolved inorganic carbon (DIC) to the coastal ocean. Between 42 and 48% of the total mangrove-derived DIC flux into the rivers, was emitted to the atmosphere, with the remaining being discharged to the coastal ocean. Dissolved organic carbon (DOC) represented ca. 10% of the total mangrove-derived dissolved carbon flux from the forests, to
25 the rivers. The sum of mangrove-derived DIC and DOC export from the forest to these rivers was estimated to be at least 18.9 to 24.5 mmol m⁻² d⁻¹, a rate lower than other independent estimates from Shark River and from other mangrove forests. Results from these experiments also suggest that in Shark and Harney Rivers, mangrove contribution to the estuarine flux of dissolved carbon to the ocean is less than 10%.

Deleted: from all sources (i.e., freshwater wetlands, mangrove, carbonate dissolution, and marine input)

Deleted: as

Deleted: Of

Deleted: dissolved inorganic carbon (DIC) exported from the forests

Deleted: these

Deleted: , between 42 and 48%

Deleted: export

Deleted: .

Deleted: this region

1 Introduction

In many tropical and sub-tropical regions, mangrove forests are a typical feature surrounding estuaries (Twilley et al., 1992; Bouillon et al., 2008a). Mangroves are thought to play an important role in tropical and subtropical coastal biogeochemical cycling and the global coastal carbon budget, due to their high productivity and rapid cycling of organic and inorganic carbon (Twilley et al., 1992; Jennerjahn and Ittekkot, 2002; Dittmar et al., 2006). However, there remain uncertainties regarding the fate of mangrove-fixed carbon and the amount of carbon exported to the coastal waters from these ecosystems (Bouillon et al., 2008a; Bouillon et al., 2008b; Kristensen et al., 2008).

Bouillon et al. (2008a) showed that over 50% of the carbon fixed by mangroves through photosynthesis could not be accounted for by growth in biomass, accumulation in soils, and export of organic carbon, and suggested that a large fraction of this missing organic carbon may be mineralized to dissolved inorganic carbon (DIC) and either lost to the atmosphere or exported to the surrounding waters. In fact, several studies have shown that the lateral advective transport of interstitial waters through tidal pumping represents a major carbon export pathway from mangroves into adjacent waters, both for DIC (Koné and Borges, 2008; Miyajima et al., 2009; Maher et al., 2013) and dissolved organic carbon (DOC) (Dittmar and Lara, 2001; Bouillon et al., 2007c). However, to date, lateral mangrove derived aquatic carbon fluxes (as a proportion of overall forest carbon mass balance) have only been estimated for short time periods and over limited spatial (e.g., plot) scales (e.g., Troxler et al., 2015). These studies also typically do not determine the fate of mangrove-derived carbon once it is exported from the forest through tidal pumping and drainage. Additional measurements of the magnitude and fate of mangrove carbon export at the basin scale are needed to help quantify connections between inter-tidal, estuarine and coastal ocean carbon cycles.

Rates of lateral dissolved carbon export from tidal mangrove forest are heterogeneous over space and time due to variability in inundation patterns, forest structure, topography, and soil hydraulic properties. Direct, plot-scale measurements of dissolved carbon export therefore may not represent rates quantified at the basin-scale. However, mangrove-derived dissolved carbon fluxes may be estimated in some systems using information on the spatial distribution of carbon-related measurements in adjacent waters. For example, the carbon balance of tidal riverine systems adjacent to mangrove forests should integrate the spatial and temporal variability of these lateral fluxes.

The objective in the study is to quantify dissolved carbon source-sink dynamics in a subtropical estuary dominated by two tidal rivers, the Shark and Harney Rivers in Everglades National Park, Florida, USA. These rivers

- Deleted: Basin-scale rates
- Deleted: advective
- Deleted: a
- Deleted: difficult to measure, because these fluxes are
- Deleted: large

are centrally-located within the largest contiguous mangrove forest in North America and they discharge to the Gulf of Mexico. The total dissolved carbon inventories and fluxes in these rivers are determined using a series of discrete and continuous measurements of carbon-related parameters along a salinity gradient, and the mangrove contribution separated using measurements of stable isotopic composition of dissolved organic and inorganic carbon. The results are then scaled by the area of mangrove forest that surrounds these rivers to express dissolved carbon fluxes on an aerial basis for comparison to independent measurements of dissolved carbon fluxes from this forest.

2 Methods

2.1 Study site

The tidal-dominated Shark and Harney Rivers (river and estuary are used interchangeably in this contribution) are surrounded by mangrove forests and located on the southwest coast of Florida (Fig. 1), within Everglades National Park. The subtropical climate in southern Florida is characterized by a May to October wet season, when approximately 60% of the annual precipitation occurs (Southeast Regional Climate Center, <http://www.sercc.com>). The Shark and Harney Rivers together discharge approximately 50% of the flow from the Shark River Slough (SRS), the primary drainage feature of Everglades National Park, to the Gulf of Mexico (GOM) (Levesque, 2004). Seasonal variation of the water discharge from SRS mostly follows the precipitation patterns (Saha et al., 2012), and influences the transport of nutrients to the mangrove ecotone (Rivera-Monroy et al., 2011). The Shark and Harney Rivers are each approximately 15 km long, and connected in Tarpon Bay (Fig. 1). The mean depths of Tarpon Bay, Shark River, and Harney River at mid tide are 1.4 ± 0.3 , 2.8 ± 0.4 , and 2.6 ± 0.4 m (Ho et al., 2014), respectively, and the surface areas are 1.48×10^6 , 2.54×10^6 , and 2.75×10^6 m², respectively. The inter-tidal zones bordering the Shark and Harney Rivers are dominated by *Rhizophora mangle* (red mangrove), *Avicennia germinans* (black mangrove), *Laguncularia racemosa* (white mangrove), and *Conocarpus erectus* (buttonwood). Semi-diurnal tides in this region inundate the forest as often as twice a day. River discharge to the GOM is primarily influenced by tides, wind, and freshwater inflow from SRS (Levesque, 2004).

Discharges are determined by the US Geological Survey at stations near the midpoints of Shark River (USGS 252230081021300 Shark River) and Harney River (USGS 252551081050900 Harney River) (Fig. 1). Discharges are generally lower during March-May than the rest of the year. Hourly mean residual discharge values (i.e., filtered for tides) from March to May of the 5-year period from 2007 to 2011 ranged from -21.9 to 24.1 m³ s⁻¹, with a mean of 0

$\text{m}^3 \text{s}^{-1}$ for Shark River, and ranged from -28.9 to $38.5 \text{ m}^3 \text{ s}^{-1}$, with a mean of $4.4 \text{ m}^3 \text{ s}^{-1}$ for Harney River. Positive values indicate flow towards the GOM. For the rest of the year (i.e., June to February), these values ranged from -46.2 to $89.2 \text{ m}^3 \text{ s}^{-1}$, with a mean of $8.8 \text{ m}^3 \text{ s}^{-1}$ for Shark River, and -41.6 to $75.0 \text{ m}^3 \text{ s}^{-1}$, with a mean of $11.3 \text{ m}^3 \text{ s}^{-1}$ for Harney River.

2.2 Shark River Tracer Release Experiments

Two field studies were conducted as part of the Shark River Tracer Release Experiment (SharkTREx 1: 20 to 25 November 2010; SharkTREx 2: 10 to 15 November 2011; (Ho et al., 2014)). The mean residual discharges for Shark River were 6.9 (hourly range: -2 to 19.9) and 4.9 (hourly range: -18.9 to 34.8) $\text{m}^3 \text{ s}^{-1}$, during SharkTREx 1 and 2, respectively, and those for Harney River were 6.0 (hourly range: -1.6 to 22.8) and 1.9 (hourly range: -17.3 to 30.6) $\text{m}^3 \text{ s}^{-1}$, during SharkTREx 1 and 2, respectively (U.S. Geological Survey, 2016).

During both campaigns, an inert tracer (sulfur hexafluoride; SF_6) was injected in the river near the point where the rivers diverge just downstream of Tarpon Bay (25.4092 , -81.0083) to determine the rates of longitudinal dispersion, and the water residence time. Each day, longitudinal surveys were made along the Shark and Harney Rivers from Tarpon Bay to the GOM, and included continuous underway measurements of temperature, salinity, SF_6 , dissolved O_2 (DO; $\mu\text{mol kg}^{-1}$), and partial pressure of CO_2 (pCO_2 ; μatm), and discrete measurements of total alkalinity (TAlk; $\mu\text{mol kg}^{-1}$), dissolved inorganic carbon (DIC; $\mu\text{mol kg}^{-1}$), dissolved organic carbon (DOC; $\mu\text{mol kg}^{-1}$), stable carbon isotopic composition of DIC and DOC ($\delta^{13}\text{C}_{\text{DIC}}$ and $\delta^{13}\text{C}_{\text{DOC}}$, respectively; ‰).

2.3 Discrete measurements

During SharkTREx 1, three to five surface water samples were collected daily in the Shark River with a 5-L Niskin bottle at ~ 0.5 m below the surface for the analysis of TAlk, DOC, $\delta^{13}\text{C}_{\text{DIC}}$, and $\delta^{13}\text{C}_{\text{DOC}}$. At each sampling site, vertical profiles of temperature, salinity, and DO were recorded using a conductivity, temperature, and depth sonde (Sea-Bird SBE 19plus V2) equipped with a Clark type polarographic O_2 sensor (SBE 43). These profiles showed that the water column was vertically well mixed. No discrete samples were collected in the Harney River during SharkTREx 1. During SharkTREx 2, discrete samples for DIC, TAlk, DOC, $\delta^{13}\text{C}_{\text{DIC}}$, and $\delta^{13}\text{C}_{\text{DOC}}$ were collected daily at 20 stations distributed within the Shark and Harney Rivers (Fig. 1).

2.3.1 Total alkalinity and dissolved inorganic carbon

125 During SharkTREx 1, samples for TAlk were collected in 250 mL HDPE bottles after passing through a 0.45
µm filter. They were stored on ice for transport to the laboratory at FIU, where TAlk was determined at room
temperature using an automated titrator (Brinkman Titrino 751) with 0.1 N HCl to a pH of 2. TAlk was calculated
130 from the volume of acid added at the inflection point closest to a pH of 4, and reported as $\mu\text{mol L}^{-1} \text{HCO}_3^-$ since the
original pH of the water samples was near neutral. The precision of the measurements was $\pm 2\%$ from replicate analysis
($n = 5$) with an accuracy of $\pm 2\%$ as determined by analysis of certified reference material (Dickson, 2010). DIC and
pH were computed from TAlk and $p\text{CO}_2$ using the dissociation constants of Cai and Wang (1998) for estuarine waters.

Deleted: meq

Deleted: DIC and pH were computed from TAlk and $p\text{CO}_2$ using the dissociation constants of (Millero, 2010) for estuarine waters.

135 During SharkTREx 2, samples for TAlk and DIC were collected in 550 mL borosilicate glass bottles,
poisoned with HgCl_2 , and sealed with hydrocarbon grease (Apiezon M). The samples were stored at room temperature
in the dark for travel to the laboratory at NOAA/AOML. Samples for TAlk were measured in an open thermostated
cell (25 °C) with an automated titrator (Metrohm 765 Dosimat) connected to a pH glass-reference electrode system
140 (Orion), using 0.2 M HCl as a titrant, and determined from the equivalence point of the titration curve using a non-
linear least-squares fit. For DIC analysis, water samples were first acidified to convert all the carbonate species to CO_2
in a DIC analyzer (Apollo SciTech), and then measured with a NDIR detector (LI-COR LI-7000). Calibrations for
DIC and TAlk were performed using certified reference material (Dickson, 2010). The analytical uncertainty of the
DIC and TAlk measurements based on replicate samples are 0.1 and 0.2%, respectively.

145 The measured TAlk and $p\text{CO}_2$ from SharkTREx 2 were used to calculate DIC using CO2SYS (Pierrot et al.,
2006) and the dissociation constants of Cai and Wang (1998), and the results were $1.3 \pm 1.1\%$ (mean \pm s.d.; $n = 77$;
range: -2.4 to +4.4%) higher than the measured DIC, possibly indicating a slight contribution (ca. 1%) to TAlk from
organic or particulate material, as the samples were not filtered.

Deleted: (Millero, 2010), and the results were $1.3 \pm 1.1\%$ (

2.3.2 Dissolved organic carbon

145 The samples analyzed for DOC were filtered with pre-combusted 0.7 µm GF/F filters and collected in pre-
cleaned, acid-washed, brown high-density polyethylene bottles (HDPE; Nalgene). Containers were rinsed three times
before sample collection, transported on ice to the FIU SERC Nutrient Analysis Lab, and stored in a refrigerator until
analyses within three weeks of collection. DOC was measured using the high-temperature catalytic combustion
method on a total organic carbon analyzer (Shimadzu TOC-V), and standardized using 10, and 50 ppm of potassium

Deleted:).

155 [hydrogen phthalate \(KHP\), with reagent water as a blank. The analytical precision based on replicates of KHP is ca. ±0.3 ppm.](#)

2.3.3 Stable carbon isotopic composition

160 Samples for $\delta^{13}\text{C}_{\text{DIC}}$ were collected in 40 ml glass bottles after passing the sample through a GF/F filter, and then poisoning with HgCl_2 . In the laboratory at RSMAS, vials with 0.5 ml 103% H_3PO_4 were flushed for 60 s with He. Approximately 2 ml of sample were then injected into the vial, and after sonification the accumulated CO_2 was analyzed by a gas chromatograph (GC) coupled to an isotope ratio mass spectrometer (GC-IRMS; Thermo Delta V). The $\delta^{13}\text{C}$ was calibrated using two standards of NHCO_3 with differing $\delta^{13}\text{C}$ values dissolved in H_2O whose isotopic compositions had been previously calibrated relative to NBS-19 using conventional dual inlet mass spectrometry (Finnigan-MAT 251). The $\delta^{13}\text{C}$ values are reported relative to the Vienna Pee Dee Belemnite (VPDB) standard, [and has a reproducibility of ±0.2 ‰ as determined by repeated analysis of internal DIC standards.](#)

165 Samples for $\delta^{13}\text{C}_{\text{DOC}}$ were collected in 60 ml brown HDPE bottles and stored on ice until returned to the lab at FIU. $\delta^{13}\text{C}_{\text{DOC}}$ samples were filtered with GF/F (0.7 μm) filter, and then stored in pre-cleaned 40 ml bottles until analyses. Measurements for $\delta^{13}\text{C}_{\text{DOC}}$ were made using a total organic carbon (TOC) analyzer (Aurora 1030W, OI Analytical) coupled to a cavity ring-down spectroscopy system (CRDS; G1111-i, Picarro) following the approach of
170 Ya et al. (2015). DIC was removed by adding H_3PO_4 and sparging with N_2 . 1.5 ml of sample was chemically oxidized to CO_2 at a temperature of 98°C in the presence of sodium persulfate ($\text{Na}_2\text{S}_2\text{O}_8$). The CO_2 generated was detected by non-dispersive infrared absorption (NDIR) for determination of DOC. The CO_2 was collected in a gas-tight bag and then pulsed into the CRDS for the $\delta^{13}\text{C}$ measurement. [In order to measure the different isotopic ranges within the collected samples, an isotopic calibration was based on two external standards of potassium hydrogen phthalate \(KHP -29.8‰, OI-Analytical\) and glutamine \(-11.45‰, Fisher\) with a concentration range of 0-25 ppm. These standards were prepared in synthetic seawater to match the salinity of the sample matrix. The isotope values of these two standards were determined by using an elemental analyzer isotope ratio mass spectrometer \(EA-IRMS\).](#) Analytical
175 precision based on replicated standards ranged from ±0.15 to ±1.52 ‰ for this study.

2.4 Underway measurements

180 Surface water was continuously pumped from an intake located near the bow of the boat at a water depth of approximately 1 m during tracer recovery operations. Water temperature and salinity were continuously recorded using a thermosalinograph (SBE 45 MicroTSG). During SharkTREx 1, DO was measured underway with a membrane covered galvanic sensor (WTW Cellox 325) calibrated with saturated air. During SharkTREx 2, DO was measured using an oxygen optode (Aanderaa 3835) calibrated against Winkler titration.

185 Underway measurements of atmospheric and waterside pCO_2 were made. Waterside pCO_2 were obtained with a showerhead type equilibrator coupled to a non-dispersive infrared (NDIR) analyzer (LI-COR 840A). Measurements of underway SF_6 were made with an automated SF_6 analysis system (Ho et al., 2002), [which is](#)

Deleted: phosphoric acid

Deleted: gas

Deleted: .

comprised of gas extraction (membrane contactor), separation (molecular sieve 5A), and detection units (gas chromatograph equipped with an electron capture detector). Both the underway pCO₂ and SF₆ measurements are described in greater detail in Ho et al. (2014)

Deleted: of these

Deleted: have been

2.5 Inventories of DIC, DOC and DO

195 The inventories of DIC, DOC and DO were calculated in the same way that SF₆ inventories were determined in Ho et al. (2014). The river was divided into 100-m longitudinal sections, and the measured concentrations, corrected for tidal movement to slack before ebb for each day, were assigned to each section *i* and then summed over the entire length of the river. For example, to calculate the inventory of DIC, denoted $\Sigma[\text{DIC}]_{\text{observed}}$ (mol):

$$\Sigma[\text{DIC}]_{\text{observed}} = \sum_{i=1}^n [\text{DIC}]_i \times V_i, \quad (1)$$

200 where $[\text{DIC}]_i$ is the mean concentration (mol L⁻¹) in section *i*, V_i is the volume of the river (L) in section *i* at mid-tide, and *n* is the number of sections in each river (*n* = 273 for Shark River and Tarpon Bay; *n* = 152 for Harney River). DOC and DO inventories were also calculated using Eq. (1), by substituting $[\text{DOC}]_i$ or $[\text{DO}]_i$ for $[\text{DIC}]_i$, accordingly.

The inventories of DIC and DOC were separated into contributions from estuarine and non-estuarine sources, first by determining inventories for DIC assuming conservative mixing between the freshwater and marine end members and then subtracting these inventories from the total observed inventories. The estuarine DIC inventory, $\Sigma[\text{DIC}]_{\text{estuary}}$, representing the DIC from all estuarine sources, was calculated as follows:

$$\Sigma[\text{DIC}]_{\text{estuary}} = \Sigma[\text{DIC}]_{\text{observed}} - \Sigma[\text{DIC}]_{\text{conserv}} + \Sigma[\text{DIC}]_{\text{gasex}}, \quad (2)$$

210 where $\Sigma[\text{DIC}]_{\text{conserv}}$ is the inventory of DIC assuming conservative mixing between freshwater and marine end members (i.e., from non-estuarine sources), and $\Sigma[\text{DIC}]_{\text{gasex}}$ is the inventory of DIC lost to air-water gas exchange from the estuary, due to pCO₂ in the water being above solubility equilibrium with the atmosphere (see section 2.6). The freshwater and marine end-members were assigned to the values measured at the lowest (Tarpon Bay) and highest salinities, respectively.

The total O₂ deficit in Shark River during the experiments was determined by examining the difference in O₂ inventories for conservative mixing and actual measurements, correcting for O₂ influx due to gas exchange using a formulation similar to Eq. (2) above (i.e., $\Sigma[\text{DO}]_{\text{deficit}} = \Sigma[\text{DO}]_{\text{conserv}} - \Sigma[\text{DO}]_{\text{observed}} + \Sigma[\text{DO}]_{\text{gasex}}$).

2.6 Air-water O₂ and CO₂ fluxes

To enable comparison between different gases and different aquatic environments, it is customary to normalize gas transfer velocities to a Schmidt number (Sc ; kinematic viscosity of water divided by diffusion coefficient of gas in water) of 600, $k(600)$, corresponding to that of CO₂ in freshwater at 20 °C. $k(600)$ for SharkTREx 1 and 2, determined from the [wind speed and current velocity](#) parameterization proposed in Ho et al. (2016), were 3.5 ± 1.0 and 4.2 ± 1.8 cm h⁻¹, respectively. To determine k for O₂ and CO₂ at the temperature and salinity measured in the rivers, the following equation was used, assuming a $Sc^{-1/2}$ scaling (Jähne et al., 1987):

$$k_{O_2} = k(600) \left(\frac{Sc_{CO_2}}{600} \right)^{-1/2}, \quad (3)$$

where k and Sc of CO₂ could be substituted in Eq. (3) for O₂, and Sc for O₂ and CO₂ were calculated as a function of temperature and salinity using data compiled by Wanninkhof (2014).

Air-water O₂ fluxes (F_{O_2} ; mmol m⁻² d⁻¹) were calculated as follows:

$$F_{O_2} = k_{O_2} (O_{2_{equil}} - O_2), \quad (4)$$

where k_{O_2} (cm h⁻¹) is the gas transfer velocity for O₂, $O_{2_{equil}}$ (mmol m⁻³) is the equilibrium concentration of O₂ in the water at a given temperature and salinity (Garcia and Gordon, 1992), and O_2 is the measured oxygen concentration in the water.

Similarly, air-water CO₂ fluxes (F_{CO_2} ; mmol m⁻² d⁻¹), which were used to determine changes in DIC due to gas exchange, were calculated as follows:

$$F_{CO_2} = k_{CO_2} K_0 \Delta pCO_2, \quad (5)$$

where k_{CO_2} (cm h⁻¹) is the gas transfer velocity for CO₂, K_0 (mol atm⁻¹ m⁻³) is the aqueous-phase solubility of CO₂ (Weiss, 1974), and ΔpCO_2 (μatm) is the difference between the measured pCO₂ in air equilibrated with water and atmospheric pCO₂.

As with the inventories, F_{CO_2} were separated into estuarine and non-estuarine contributions. Because of the non-linearity in the relationship between pCO₂ and other carbonate system parameters, the pCO₂ in the river expected from conservative mixing was calculated by assuming conservative mixing for DIC and TALK, and then calculating pCO₂ using CO2SYS (Pierrot et al., 2006), with the dissociation constants of [Cai and Wang \(1998\)](#). Then, the non-estuarine F_{CO_2} was calculated as above with Eq. (5), and the F_{CO_2} attributed to estuarine sources was determined as the difference between total and non-estuarine F_{CO_2} .

Deleted: Millero (2010).

2.7 Estuarine and mangrove contributions to DIC

DIC in the Shark and Harney Rivers may originate from several sources in addition to input from the freshwater marsh upstream and the coastal ocean, including: 1) mangrove root respiration; 2) organic matter mineralization in sediments or in river water; 3) dissolution of CaCO_3 in sediments or in river water; and 4) groundwater discharge. Groundwater in this region is likely to contain DIC from CaCO_3 dissolution that occurs when saltwater intrudes into the karst aquifer that underlies this region (Price et al., 2006), as well as DIC from sediment organic matter mineralization. In this setting, the combination of #1 and #2 represents the mangrove source of DIC ($[\text{DIC}]_{\text{mangrove}}$), and the combination of #3 and #4 represents the CaCO_3 dissolution source ($[\text{DIC}]_{\text{dissolution}}$) to estuarine [DIC]:

$$[\text{DIC}]_{\text{estuary}} = [\text{DIC}]_{\text{observed}} - [\text{DIC}]_{\text{conserv}} + [\text{DIC}]_{\text{gasex}} = [\text{DIC}]_{\text{mangrove}} + [\text{DIC}]_{\text{dissolution}} \quad (6)$$

where $[\text{DIC}]_{\text{observed}}$ is the observed DIC concentration, $[\text{DIC}]_{\text{conserv}}$ is the DIC concentration expected by conservative mixing of the two end-members, and $[\text{DIC}]_{\text{gasex}}$ is the correction for change in $[\text{DIC}]_{\text{observed}}$ due to loss through air-water gas exchange as the water transits through the estuary. $[\text{DIC}]_{\text{gasex}}$ was determined from F_{CO_2} and the residence time of water during each experiment (Ho et al., 2016).

Measurements of $\delta^{13}\text{C}_{\text{DIC}}$ and estuarine DIC/Talk ratios were used to determine the mangrove sources to estuarine DIC. Fixation of CO_2 through photosynthesis is neglected in both models as these rivers are characterized by low chlorophyll-*a* concentration and low phytoplankton biomass (Boyer et al., 1997). During SharkTReX 1 and 2, there was a negligible difference between pCO_2 measured during the day and night (ca. 3%).

2.7.1 Determining mangrove contribution from $\delta^{13}\text{C}_{\text{DIC}}$

Processes 1 through 4 listed above influence $\delta^{13}\text{C}_{\text{DIC}}$ in the estuary differently due to the differences in the $\delta^{13}\text{C}$ values originating from respiration of mangrove-derived organic matter, and CaCO_3 dissolution. The isotopic fractionation during respiration of organic matter is small, and the $\delta^{13}\text{C}_{\text{DIC}}$ values produced via this pathway should be approximately equivalent to the $\delta^{13}\text{C}$ of the organic matter respired (DeNiro and Epstein, 1978). The isotopic fractionation during dissolution/re-precipitation of CaCO_3 is also considered to be negligible (Salomons and Mook, 1986).

The expected $\delta^{13}\text{C}$ values of DIC in the rivers as a result of conservative mixing ($\delta^{13}\text{C}_{\text{conserv}}$) of the marine and freshwater end-members of the Shark and Harney Rivers were calculated as follows (Mook and Tan, 1991):

$$275 \quad \delta^{13}C_{conserv} = \frac{S([DIC]_F \delta^{13}C_F - [DIC]_M \delta^{13}C_M) + S_F [DIC]_M \delta^{13}C_M - S_M [DIC]_F \delta^{13}C_F}{S([DIC]_F - [DIC]_M) + S_F [DIC]_M - S_M [DIC]_F}, \quad (7)$$

where [DIC] is the observed DIC concentration, S is the measured salinity, and M and F subscripts refer to the marine and freshwater end-members, respectively.

An estimate of the maximum contribution of $[DIC]_{mangrove}$ and $[DIC]_{dissolution}$ to $[DIC]_{estuary}$ can be obtained by solving Equations 6 and 8:

$$280 \quad \delta^{13}C_{DIC} \times [DIC]_{observed} = \delta^{13}C_{conserv} \times [DIC]_{conserv} + \delta^{13}C_{mangrove} \times [DIC]_{mangrove} + \delta^{13}C_{dissolution} \times [DIC]_{dissolution} - \left(\delta^{13}C_{DIC} - \epsilon_{13C_{DIC-CO_2}} \right) \times [DIC]_{gaseq}, \quad (8)$$

where the $\delta^{13}C_{conserv}$ value is the DIC isotopic composition expected for conservative mixing (Mook and Tan, 1991),

$\delta^{13}C_{mangrove}$ is the isotopic composition for mangrove-derived material (-30‰; Mancera-Pineda et al., 2009), the

$\delta^{13}C_{dissolution}$ value is the $\delta^{13}C$ composition of calcite (~1‰), and $\epsilon_{13C_{DIC-CO_2}}$ is the equilibrium isotope fractionation

285 between DIC and CO_2 gas (~-8‰; Zhang et al., 1995).

2.7.2 Determining mangrove contribution from TALK/DIC

An independent approach to separate the mangrove contribution from $CaCO_3$ dissolution is to use the co-variation of $[DIC]_{estuary}$ and $[TALK]_{estuary}$ as an indicator of the biogeochemical processes affecting DIC dynamics (Borges et al., 2003; Bouillon et al., 2007c), as these processes have different effects on DIC and TALK. Assuming
290 that $[TALK]_{estuary}$ is mainly produced by the dissolution of $CaCO_3$, $[DIC]_{dissolution}$ can be determined as $0.5 \times [TALK]_{estuary}$, and then $[DIC]_{mangrove}$ can be calculated from Eq. (6). However, since sulfate reduction, a primary mineralization pathway in mangrove sediments, may also contribute to [TALK] (Alongi, 1998; Alongi et al., 2005) this calculation represents an upper bound estimate for $[DIC]_{dissolution}$ and a lower bound estimate for $[DIC]_{mangrove}$.

2.8 Determining mangrove contribution to DOC

295 In the Shark and Harney Rivers, dissolved organic matter may be derived from upstream freshwater wetland species such as periphyton and sawgrass, from seagrass communities and marine phytoplankton, or from mangrove vegetation inside the estuary (Jaffe et al., 2001). The estuarine contributions to DOC ($[DOC]_{estuary}$) in the rivers was determined in the same way as for DIC above using Eq. (6), by substituting DOC for DIC accordingly, without the correction for gas exchange:

$$300 \quad [DOC]_{estuary} = [DOC]_{observed} - [DOC]_{conserv}, \quad (9)$$

where $[\text{DOC}]_{\text{observed}}$ is the observed DOC concentration, $[\text{DOC}]_{\text{conserv}}$ is the DOC concentration expected from conservative mixing of the two end-members.

Then, measurements of $\delta^{13}\text{C}_{\text{DOC}}$ were made to ascertain the mangrove source of DOC in the river, in order to determine the proportion of $[\text{DOC}]_{\text{estuary}}$ that is of mangrove origin. The expected $\delta^{13}\text{C}$ values of DOC as a result of conservative mixing ($\delta^{13}\text{C}_{\text{conserv}}$) were calculated using Eq. (7), substituting DOC for DIC. Assuming that $[\text{DOC}]_{\text{estuary}}$ was entirely mangrove-derived, $[\text{DOC}]_{\text{mangrove}}$ should equal:

$$[\text{DOC}]_{\text{mangrove}} = \frac{[\text{DOC}]_{\text{observed}}\delta^{13}\text{C}_{\text{DOC}} + [\text{DOC}]_{\text{conserv}}\delta^{13}\text{C}_{\text{conserv}}}{\delta^{13}\text{C}_{\text{mangrove}}}, \quad (10)$$

where $\delta^{13}\text{C}_{\text{mangrove}}$ is the isotopic composition for mangrove-derived material (-30‰).

2.9 Longitudinal dispersion

The longitudinal SF_6 distribution was corrected for tidal movement to slack water before ebb for each day using a method described in Ho et al. (2002). The absolute magnitudes of the average daily corrections were 2.0 and 2.7 km for SharkTREx 1 and 2, respectively, with a range for individual measurements of 0 to 5.8 km and 0 to 7.3 km for SharkTREx 1 and 2, respectively. Longitudinal dispersion coefficient K_x ($\text{m}^2 \text{s}^{-1}$) was calculated from the change of moment of the longitudinal SF_6 distribution over time as follows (Fischer et al., 1979; Rutherford, 1994):

$$K_x = \frac{1}{2} \left(\frac{d\sigma_x^2}{dt} \right), \quad (11)$$

where σ_x^2 is the second moment of the longitudinal SF_6 distribution for each day.

2.10 Longitudinal fluxes to the Gulf of Mexico

The longitudinal fluxes of DIC and DOC from Shark and Harney Rivers to the Gulf of Mexico were calculated using the averaged DIC or DOC inventories, and the residence time of water (τ ; d), which was determined from the decrease in the inventory of SF_6 after correcting for air-water gas exchange (Ho et al., 2016). For example, the longitudinal DIC flux (F_{DIC} ; mol d^{-1}) can be calculated as follows:

$$F_{\text{DIC}} = \frac{\Sigma[\text{DIC}]_{\text{observed}}}{\tau}. \quad (12)$$

Equation (12) can be used to calculate the fluxes of any other dissolved or suspended substance in the river by substituting its inventory in place of DIC. In addition, using the estuarine and non-estuarine fractions of the inventories in equation (12) allowed the estuarine and non-estuarine proportions of the longitudinal carbon fluxes to be quantified.

The advantage of this method to calculate longitudinal flux in a tidal river over a method that uses net discharge and constituent concentration is that the effect of tidal flushing is implicitly accounted for by the residence

Deleted: As with

Deleted: inventory calculations, longitudinal fluxes were separated into

Deleted: contributions

time, and therefore there is not a need to explicitly define the fraction of river water in the return flow during each flood tide.

3 Results and Discussion

3.1 Distribution patterns and carbon inventories

During SharkTREx 1, the salinity along the longitudinal transects ranged from 1.2 to 27.1, and the mean (\pm s.d.) water temperature was 23.4 ± 0.2 °C (n = 3767). During SharkTREx 2, salinity ranged from 0.6 to 27.1, and water temperatures averaged 22.7 ± 0.9 °C (n = 3818).

Deleted: .

Deleted: .

Both pCO₂ and DO showed large spatial variability within the Shark and Harney Rivers during SharkTREx 1 and 2 (Fig. 2). Measured pCO₂ values were well above atmospheric equilibrium along the entire salinity range, with values ranging from ca. 1000 to 6200 μ atm. Maximum pCO₂ values were observed at intermediate salinities, decreasing towards both end-members, while DO showed the opposite pattern, with saturations ranging from 36 to 113%.

The patterns of TALK and DIC along the salinity gradient followed the same trend as pCO₂ and were clearly non-conservative (Fig. 3a-f). TALK varied between ca. 3400 and 5000 μ mol kg⁻¹ during SharkTREx 1 and between ca. 3000 and 3900 μ mol kg⁻¹ during SharkTREx 2. DIC ranged from ca. 3400 to 5100 μ mol kg⁻¹ during SharkTREx 1, and ca. 2800 to 4000 μ mol kg⁻¹ during SharkTREx 2. $\delta^{13}\text{C}_{\text{DIC}}$ values ranged from -10.3 to -6.6 ‰ and from -11.4 to -5.8 ‰ during SharkTREx 1 and 2, respectively. Higher DIC, TALK and pCO₂ coincided with lower O₂ saturation, more depleted $\delta^{13}\text{C}_{\text{DIC}}$, and lower pH values (Fig. 3g-i), indicative of mineralization of mangrove-derived organic matter within the estuary.

Deleted: A negative correlation was observed between $\delta^{13}\text{C}_{\text{DIC}}$ and both DIC and pCO₂ values, demonstrating that the source of estuarine DIC was depleted in ¹³C.

During SharkTREx 1, the DOC concentrations in the freshwater end member were higher than SharkTREx 2 (Fig. 4). For both experiments, DOC concentrations followed a non-conservative pattern (see also Cawley et al., 2013), but this trend was less apparent during SharkTREx 1 compared to SharkTREx 2 (Fig. 4).

The inventories of DIC, DOC, DO, TALK, and pCO₂ were relatively constant in the Shark and Harney Rivers, indicating quasi steady state conditions during SharkTREx 1 and 2. Under these conditions, carbon inputs and exports are balanced, and fluxes and concentrations may be examined interchangeably. K_1 during the experiments (16.4 ± 4.7 and 77.3 ± 6.5 m² s⁻¹ for Shark River during SharkTREx 1 and 2, respectively, and 136.1 ± 16.5 m² s⁻¹ for Harney

River during SharkTREx 2) were relatively large, and suggest that any perturbations (such as export of DIC from mangroves) would be quickly mixed thoroughly in the estuary.

365 In the following, for brevity, fluxes and inventories are summarized as ranges, which cover the two rivers and two experiments so they reflect both temporal and spatial variability. The individual values are given in Tables 1 and 2.

DIC was the dominant form of dissolved carbon in both rivers and accounted for 79 to 82% of the total dissolved carbon in the rivers. The contribution of DOC to the total carbon pool varied between 18 and 21% (Table 370 1).

3.2 Air-water CO₂ fluxes

As shown by Ho et al. (2014), pCO₂ observed during SharkTREx 1 and 2 fall in the upper range of those reported in other estuarine (Borges, 2005) and mangrove-dominated systems (Bouillon et al., 2003; Bouillon et al., 2007a; Bouillon et al., 2007b; Koné and Borges, 2008; Call et al., 2015). The mean air-water CO₂ fluxes in Shark 375 River for SharkTREx 1 and 2 were 105 ± 9 and 99 ± 6 mmol m⁻² d⁻¹ (Ho et al., 2016). The analysis is taken further here by including data from Harney River. The mean air-water CO₂ fluxes in Harney River were 150 ± 8 and 114 ± 21 mmol m⁻² d⁻¹ for SharkTREx 1 and 2, respectively.

Borges et al. (2003) summarized all available pCO₂ data from mangrove surrounding waters, and calculated CO₂ fluxes to the atmosphere that averaged 50 mmol m⁻² d⁻¹ (with a range of 4.6 to 113.5 mmol m⁻² d⁻¹), and Bouillon 380 et al. (2008a) estimated a global CO₂ flux from mangroves of ca. 60 ± 45 mmol m⁻² d⁻¹. One reason that the fluxes from SharkTREx 1 and 2 are on the upper end of those estimates may be that the Shark and Harney Rivers receive a large input of DIC from the freshwater marsh upstream (Table 1), causing higher pCO₂ in the estuary compared to the global average.

Scaling the air-water CO₂ fluxes by the area of open water in the Shark and Harney Rivers, where Tarpon 385 Bay is included with Shark River, suggests that the total carbon emissions to the atmosphere through air-water gas exchange in Shark River was $4.2 \pm 0.4 \times 10^5$ and $4.0 \pm 0.2 \times 10^5$ mol d⁻¹ during SharkTREx 1 and 2, respectively, and were $4.1 \pm 0.2 \times 10^5$ and $3.1 \pm 0.6 \times 10^5$ mol d⁻¹ from the Harney River during SharkTREx 1 and 2, respectively (Fig. 5), which is remarkably consistent, both spatially and temporally.

These fluxes were incorporated into the DIC mass balance of the Shark and Harney Rivers (Eq. 2) by 390 calculating the total CO₂ degassed over the residence time of water in the rivers. Given the mean air-water CO₂ fluxes

Deleted: ,

(Table 2), the total CO₂ degassed in the Shark River represents approximately 13 and 21% of $\Sigma[\text{DIC}]_{\text{observed}}$ during SharkTREx 1 and 2, respectively, and the CO₂ degassed from the Harney River during SharkTREx 2 represents 20% of $\Sigma[\text{DIC}]_{\text{observed}}$, indicating that air-water CO₂ exchange removes a non-negligible fraction of the inorganic carbon in these rivers. Exclusion of $\Sigma[\text{DIC}]_{\text{gasex}}$ from the mass balance in Eq. (2) would lead to an underestimation of $\Sigma[\text{DIC}]_{\text{estuary}}$ of between 33 and 44%.

3.3 Mangrove contribution to DIC inventory

The highest DIC concentrations were correlated with low DO (Fig. 2) and characterized by ¹³C-depletion (Fig. 3j, k, l). Observations of elevated DIC and pCO₂ in the middle of the estuary, coupled with $\delta^{13}\text{C}_{\text{DIC}}$ and O₂ depletion may indicate the importance, noted by other authors, of lateral transport of pore water from the peat-based mangrove forest into the river via tidal pumping (Bouillon et al., 2008a; Maher et al., 2013). However, as demonstrated below, the observed DIC and $\delta^{13}\text{C}_{\text{DIC}}$ distributions in these rivers cannot be explained solely by mineralization of mangrove-derived organic carbon.

3.3.1 Evidence from $\delta^{13}\text{C}_{\text{DIC}}$

The distributions of DIC and $\delta^{13}\text{C}_{\text{DIC}}$ cannot be explained solely by the addition of mangrove-derived DIC and air-water gas exchange. Solving Eq. (8) for $\delta^{13}\text{C}_{\text{DIC}}$, assuming that $[\text{DIC}]_{\text{dissolution}}$ is negligible and that the only source of DIC in the rivers is of mangrove origin, would result in $\delta^{13}\text{C}$ values significantly lower than those observed. The low pH in interstitial waters of mangrove sediments due to organic matter mineralization processes may be favorable to CaCO₃ dissolution in mangrove sediments, and this process could have an effect on estuarine $\delta^{13}\text{C}_{\text{DIC}}$. Groundwater discharge could also influence DIC and $\delta^{13}\text{C}_{\text{DIC}}$. Inputs of DIC derived from CaCO₃ dissolution from either of these sources may explain the differences in observed $\delta^{13}\text{C}_{\text{DIC}}$ and those expected if $[\text{DIC}]_{\text{estuary}}$ was entirely of mangrove origin.

Solving Equations 6 and 8, the mineralization of mangrove-derived organic matter is estimated to account for ca. $60 \pm 6\%$ of $\Sigma[\text{DIC}]_{\text{estuary}}$ (Table 3), with the remainder originating from the dissolution of CaCO₃. This estimate is sensitive to the end member value chosen for $\delta^{13}\text{C}_{\text{mangroves}}$ and $\delta^{13}\text{C}_{\text{dissolution}}$. For instance, if $\delta^{13}\text{C}_{\text{mangroves}}$ were -29‰ instead of -30‰, the mangrove contribution would increase to 62%.

Deleted: Other recent studies have observed similar differences in pore water $\delta^{13}\text{C}_{\text{DIC}}$ values and the values expected from the carbon inputs derived from organic matter decomposition and CaCO₃ dissolution (Walter et al., 2007). In these studies, the differences were attributed to isotopic exchange during CaCO₃ dissolution and re-precipitation, and if these processes were active in the substrate or mangrove sediments surrounding the Shark and Harney Rivers, they would affect observed $\delta^{13}\text{C}_{\text{DIC}}$ values without affecting $[\text{DIC}]_{\text{estuary}}$.

425 3.3.2 Evidence from DIC and TALK

In the Shark and Harney Rivers, the high correlation ($r^2 = 0.99$; Fig. 6) between $[DIC]_{estuary}$ and $[TALK]_{estuary}$ indicates the same processes control the inputs of DIC and TALK to these rivers. By examining the covariation of $[DIC]_{estuary}$ and $[TALK]_{estuary}$, mangroves were found to contribute a minimum of $70 \pm 3\%$ of $\Sigma[DIC]_{estuary}$ (Table 3), with the remainder due to the dissolution of $CaCO_3$. These estimates are in reasonable agreement with those based on the carbon isotopic mass balance.

The $[TALK]_{estuary}$ vs. $[DIC]_{estuary}$ ratios were 0.84 and 0.92 for Shark River during SharkTREx 1 and 2, and 0.90 for the Harney River during SharkTREx 2 (Fig. 6). The TALK to DIC ratios for $CaCO_3$ dissolution, sulfate reduction, and aerobic respiration are -0.2, 0.99, and 2, respectively. Hence, in order to achieve the observed ratios, and given the estimated contribution of $CaCO_3$ dissolution to $\Sigma[DIC]_{estuary}$ of ca. 30%, sulfate reduction and aerobic respiration were estimated to contribute 32 to 39% and 31 to 38%, respectively.

Deleted: One reason why the $\delta^{13}C_{DIC}$ -based estimates might be lower is that the potential of ^{13}C isotopic exchange during $CaCO_3$ dissolution and re-precipitation is not being considered.

Deleted: Given

435 3.3.3 Evidence from DO

The deficit of O_2 in Shark River was found to be $2.7 \pm 0.7 \times 10^6$ and $3.7 \pm 0.3 \times 10^6$ mol during SharkTREx 1 and 2, respectively. Assuming a stoichiometric ratio of ca. 1.1 for O_2 to CO_2 during degradation/remineralization of terrestrial organic matter (Severinghaus, 1995; Keeling and Manning, 2014), the maximum contribution of aerobic respiration to the DIC added to the estuary was estimated to be 57 to 69%. However, O_2 may also be consumed during oxidation of reduced products from anaerobic metabolism, such as H_2S , Mn^{2+} or Fe^{2+} , with similar O_2 to CO_2 stoichiometry as aerobic respiration. Hence, the numbers derived above represent an upper limit for aerobic respiration, and if there were complete re-oxidation of metabolites from anaerobic respiration, the O_2 deficit would represent total mineralization of terrestrial organic matter instead of just aerobic respiration. The mangrove contributions estimated from $\delta^{13}C_{DIC}$ (section 3.3.1) and TALK/DIC (section 3.3.2) are consistent with this analysis of the O_2 deficit, which indicates that a minimum of 57-69% of $\Sigma[DIC]_{estuary}$ derived from the mineralization of organic matter.

445 3.4 Mangrove contributions to DOC inventory

During both experiments, the $\delta^{13}C_{DOC}$ was highly depleted, indicative of contribution from higher plants, including mangroves. During SharkTREx 1, the lowest observed $\delta^{13}C_{DOC}$ value (-31.6‰) was in the mid-estuary (i.e., from salinity of ca. 10 to 20) (Fig. 4d). Previous studies of DOC from mangrove-dominated systems have reported

Deleted: 33.8‰) was in the mid-estuary (i.e., from salinity of ca. 10 to 20) (Fig. 4d), and it was lower than mangrove-derived material, indicative of a highly reworked organic matter source, and perhaps preferential degradation of enriched compounds had resulted in further ^{13}C depletion (Hayes, 1993).

values as low as -30.4‰ (Dittmar et al., 2006), and some of the more depleted samples from SharkTREx 1 might have DOC sourced from algae associated with mangrove roots, which can have relatively depleted values (Kieckbusch et al., 2004). The overall $\delta^{13}\text{C}_{\text{DOC}}$ depletion was less during SharkTREx 2, and the overall distribution was indicative of a stronger marine influence and/or mixing (Fig. 4e, f). The marine end member had a more enriched $\delta^{13}\text{C}_{\text{DOC}}$, indicating a greater contribution of seagrass and/or marine phytoplankton derived organic matter to the marine DOC pool (Anderson and Fourqurean, 2003). These observations are consistent with the greater longitudinal dispersion observed during SharkTREx 2 compared to SharkTREx 1.

The calculations of mangrove contribution using $\delta^{13}\text{C}_{\text{DOC}}$ mass balances (Eq. 10) also suggest that the majority of $[\text{DOC}]_{\text{estuary}}$, but only a small percentage of the total DOC inventory, was derived from mangroves (7 and 5% in the Shark River during SharkTREx 1 and 2, and 7% in the Harney River during SharkTREx 2).

3.5 Longitudinal fluxes to the Gulf of Mexico and comparison with previous studies

Residence times of Shark River (including Tarpon Bay) for SharkTREx 1 and 2 were, 5.8 ± 0.4 and 8.1 ± 1.1 days, respectively (Ho et al., 2016), and that of Harney River was 4.7 ± 0.7 days for SharkTREx 2. The resulting longitudinal DIC fluxes to the Gulf of Mexico (15.8 to $33.6 \times 10^5 \text{ mol d}^{-1}$) were significantly larger than the longitudinal DOC fluxes (3.3 to $7.5 \times 10^5 \text{ mol d}^{-1}$) at salinity of ca. 27 (Fig. 5; Table 2).

There are no previously published DIC inventories or fluxes for the Shark and Harney Rivers, so comparison with previous studies is focused on the DOC results. The DOC flux from the Shark River to the coastal ocean in SharkTREx 1 ($7.5 \pm 0.2 \times 10^5 \text{ mol d}^{-1}$) is in very good agreement to that estimated by Bergamaschi et al. (2011) in an experiment conducted in the Shark River from 20-30 September 2010 ($7.6 \pm 0.5 \times 10^5 \text{ mol d}^{-1}$). However, the net discharge during the Bergamaschi et al. (2011) study was higher than SharkTREx 1 (mean \pm s.d.: 9.1 ± 7.1 vs. $6.9 \pm 5.3 \text{ m}^3 \text{ s}^{-1}$), which would lead to a shorter residence time of 4.6 days using a relationship presented in Ho et al. (2016). Using the DOC concentration data presented in Bergamaschi et al. (2011) yields an inventory that is ca. 3% higher than the DOC inventory in Shark River during SharkTREx 1. Calculations using the shorter residence time and higher DOC inventory yields a DOC flux of $9.7 \pm 0.2 \times 10^5 \text{ mol d}^{-1}$, which is ca. 30% higher than the estimates of Bergamaschi et al. (2011).

The longitudinal flux of mangrove-derived DOC from Shark River during SharkTREx 1 ($0.3 \pm 0.2 \times 10^5 \text{ mol d}^{-1}$; Table 2) is in rough agreement with the estimate of Cawley et al. (2013) during the same period ($0.2 \times 10^5 \text{ mol d}^{-1}$), but the value for Harney River ($0.6 \pm 0.6 \times 10^5 \text{ mol d}^{-1}$) is lower than their estimate ($1.6 \times 10^5 \text{ mol d}^{-1}$).

Deleted: The difference between both methods may be due to the fact that Bergamaschi et al. (2011) estimated the longitudinal flux at a location ca. 9.5 km from the mouth of the Shark River. Because the DOC concentration gradients in the middle of the estuary are higher than at the mouth, this may overestimate the flux.

Mangroves contributed 4% to 6% of the total longitudinal DOC flux in the Shark River and 7% in the Harney River during SharkTREx 2 (Tables 1 and 4). Cawley et al. (2013), estimated a mangrove contribution to DOC flux of $3 \pm 10\%$ for Shark River and $21 \pm 8\%$ for the Harney River during November 2010, the same time period as SharkTREx 1. DOC measurements were not made in Harney River as part of SharkTREx 1. However, using the November 2010 DOC data from Harney River collected by Cawley et al. (2013) for inventory calculations, along with residence time derived from the tracers, a mangrove contribution of 19% to the total DOC longitudinal flux to the Gulf of Mexico was obtained.

3.6 Distribution of carbon fluxes

During SharkTREx 1 and 2, $\Sigma[\text{DIC}]_{\text{estuary}}$ made up 20-28% of the total DIC in the rivers, and $\Sigma[\text{DOC}]_{\text{estuary}}$ made up only 4 to 7% of the total DOC in the rivers. Mangroves are estimated to contribute 13 to 19% to the total DIC inventory. In all cases, the mangrove contribution to the DIC inventory is a factor of 3 greater than the mangrove contribution to the DOC inventory (Table 1).

During SharkTREx 1 and 2, the inventory of mangrove-derived DIC exceeded that of DOC by a factor of 15 to 17, which supports the idea that a large fraction of the carbon exported by mangroves to surrounding water is as DIC (Bouillon et al., 2008a), but is considerably larger than the estimates of ca. 3 to 10 compiled by Bouillon et al. (2008a) for mangroves at 5 sites in Asia and Africa.

The total dissolved carbon fluxes from all sources (i.e., freshwater wetland, mangrove, carbonate dissolution, and marine input) out of the Shark and Harney Rivers during SharkTREx 1 and 2 are dominated by inorganic carbon (82-83%; see Tables 2 and 4), either via air-water CO_2 exchange or longitudinal flux of DIC to the coastal ocean (Fig. 5). The remaining 17-18% of the export is as DOC. This proportioning is remarkably similar between SharkTREx 1 and 2, and between the Shark and Harney Rivers (Table 1). The estuarine contribution to these fluxes is relatively small (generally <15%), with the exception of air-water CO_2 flux, where the estuary contribution was 49 to 63% (Table 4).

In this study, the particulate organic carbon (POC) flux was not examined. However, He et al. (2014) estimated the mangrove-derived POC flux in Shark River by taking the total volume discharge from the five major rivers along the southwest coast of Everglades National Park from 2004 to 2008, and assuming that Shark River contributed 14% to the mean annual discharge. They then multiplied this discharge by the average POM concentration

($5.20 \pm 0.614 \text{ mg L}^{-1}$) in the middle of the estuary to yield an annual POM flux from Shark River. Based on analysis of organic matter biomarkers, He et al. (2014) estimated that mangrove-derived POM was 70–90% of the total POM pool in the Shark River. Using this contribution and further assuming that 58% of POM weight is POC (Howard, 1965), they estimated a POC flux of 1.0 to $2.2 \times 10^4 \text{ mol d}^{-1}$. Because this estimate was based on biomarker and POM data from the mid-estuary, where the POM concentration and the mangrove contribution to POM are both likely to be much higher than either toward the freshwater end member or the marine end member, it is likely an overestimate of the mangrove derived POC flux. Nevertheless, the mangrove-derived POC flux determined by He et al. (2014) is still only a small fraction (3 to 7%) of the mangrove-derived dissolved carbon fluxes in Shark River during SharkTREx 1 and 2.

530 3.7 Mangrove contributing area and estuary carbon balance

One of the challenges of relating the results reported here to other studies is to scale the results to a mangrove contributing area, and thereby relate the findings to mangrove forest carbon balance, typically expressed on an aerial basis. Estimates of forest carbon export derived here are compared with other investigations in this estuary. The entire area of mangroves surrounding the Shark and Harney Rivers region is ca. 111 km^2 , and the water area is ca. 17.5 km^2 (Ho et al., 2014). Scaling the forest area by the water area of Shark River (2.5 km^2) yields an associated forest area of 15.9 km^2 . The forest area associated with Harney River (2.8 km^2) is 17.4 km^2 .

Using the total forest area associated with Shark River to scale estimates of total export of mangrove-derived carbon (the combination of longitudinal fluxes and air-water gas exchange) suggests an average dissolved carbon lateral export rate from the forest of 18.9 to $24.5 \text{ mmol m}^{-2} \text{ d}^{-1}$, including both DIC and DOC. However, since it is unknown what fraction of the total forest area associated with these rivers exported dissolved carbon through tidal pumping (a function of tidal height and duration), this is considered to be a minimum estimate. Average water levels at high tide during SharkTREx 1 and 2 at the USGS Shark River station were 88% and 95% of maximum wet season water levels reported at this site over the period from November 2007 to December 2012 (U.S. Geological Survey, 2016), and 12 inundation events occurred during both SharkTREx 1 and 2. Water levels in the main river channel at the USGS Shark River station were above an estimate of the average minimum ground surface elevation derived from nearby groundwater monitoring wells in the estuary (sites SH3 and SH4; <http://sofia.usgs.gov/eden/stationlist.php>) for 21% and 28% of the time during the SharkTREx 1 and 2 experimental periods, respectively. These values indicate the export of dissolved carbon from flooded portions of the forest during the discontinuous inundation periods should be

significantly greater than the dissolved carbon lateral export rate derived above in order to produce the observed
550 inventories of mangrove-derived dissolved carbon in the main channel.

Bergamaschi et al. (2011) proposed an annual total DOC export from the forest surrounding Shark River of
15.1 ± 1.1 mol m⁻² y⁻¹ and describe their method of calculating contributing area using a model based on the
relationship between discharge volume and changes in water levels during tidal cycles. They do not provide a
contributing area, but this can be calculated from their results. They determined longitudinal DOC fluxes of 7.6 ± 0.5
555 x 10⁵ and 1.3 ± 0.02 x 10⁵ mol d⁻¹ for the wet and dry seasons, respectively, and assumed that they are entirely of
mangrove origin. Given the lengths of the wet and dry seasons, this would yield a mean annual DOC flux of 3.9 ± 0.2
x 10⁵ mol d⁻¹, and 9.4 ± 0.7 km² of mangrove forest contributing to carbon fluxes thru tidal flushing in this segment
of Shark River. However, data from SharkTREx 1 and 2 indicate that ca. 5% of the total longitudinal DOC fluxes
were of mangrove origin, with an average mangrove-derived DIC to DOC flux ratio of 10.5. Using this information,
560 the Bergamaschi et al. (2011) results were recalculated to yield a wet season dissolved carbon lateral export rate of
46.5 ± 4.4 mmol m⁻² d⁻¹ (as DIC and DOC) from the forest.

Another method of estimating forest lateral carbon export utilizes the difference between measurements of
net ecosystem-atmosphere CO₂ exchange (NEE) above the mangrove forest surrounding Shark River (267 ± 15 mmol
m⁻² y⁻¹ in 2004; (Barr et al., 2012) and corresponding measures of net ecosystem carbon balance (NECB; 227 ± 14
565 mmol m⁻² d⁻¹). NECB in 2004 can be estimated as the sum of carbon in litter fall (104 ± 8 mmol m⁻² d⁻¹), wood
production (44 ± 3 mmol m⁻² d⁻¹) (Castañeda-Moya et al., 2013), root growth (47 ± 11 mmol m⁻² d⁻¹) (Castañeda-
Moya et al., 2011) and soil carbon accumulation (31.7 mmol m⁻² d⁻¹) (Breithaupt et al., 2014) measured at the same
location (FCE LTER site SRS6) in this forest. The difference between NEE and NECB (40 ± 17 mmol m⁻² d⁻¹) provides
an estimate of the annual rate of forest carbon export to Shark River on a daily basis (Chapin et al., 2006).

570 The rate of mangrove-derived carbon exported to estuarine waters is likely to vary over space and time, as a
result of factors that include tidal cycles, phenology, and forest and soil structural characteristics. For example,
Bergamaschi et al. (2011) found that DOC fluxes were 6 times higher during the wet season (September) than the dry
season (April), whereas Cawley et al. (2013) found that the DOC fluxes were 4 and 10 times higher during the wet vs.
dry season (November vs. March) in the Shark and Harney Rivers, respectively. Barr et al. (2013) showed that forest
575 respiration rates derived from NEE data are greater during the wet than dry seasons. Higher respiration rates combined
with increased inundation during the wet compared to dry seasons suggest that wet season DIC export will also be

greater than dry season values. For these reasons, the annual carbon export rates derived from the difference between NECB and NEE are expected to underestimate wet season values. If annual lateral carbon export rates are considered as equivalent to a time-weighted sum of dry season (7 months) and wet season (5 months) values (after Bergamaschi et al. 2011), and wet season export is assumed to be, for example, 5 times greater than dry season values, the seasonal export rates (15 and 75 mmol m⁻² d⁻¹ for dry and wet seasons, respectively) that correspond with the difference between annual NECB and NEE can be calculated.

The discrepancies between the estimates of carbon export rates derived here, and those derived from Bergamaschi et al. (2011) and the difference between NEE and NECB point out the need for additional studies to reduce the uncertainty in the relationships between riverine carbon fluxes, forest carbon export, and estimates of contributing areas. For example, Bergamaschi et al. (2011) conducted an Eulerian study at a single location in the middle of the estuary, where the mangrove influence might be higher than the Lagrangian study conducted during SharkTREx 1 and 2, which covered the entire estuary. Also, the estimate of forest carbon export based on the difference between NEE and NECB is from a single location along Shark River (at FCE LTER site SRS6), and may not be representative of the entire forest. Furthermore, forest lateral carbon export rates and contributing areas should be considered dynamic, varying over semi-diurnal time scales with the extent and duration of inundation during individual tidal cycles. The correct interpretation of a single, static value for contributing area such as derived above is therefore uncertain, since the tracer-based results represent an integration of carbon sources and sinks calculated over the water residence time and expressed on daily time scales. To improve understanding of how mangrove forest carbon balance and export influence riverine carbon inventories and fluxes to the Gulf of Mexico in this system, wet and dry season measurements over multiple years, information on the relationships between forest structure, productivity and lateral carbon export rates, and independent estimates of forest inundation area in relation to tidal height are needed.

4 Conclusions

The SharkTREx 1 and 2 studies are the first to provide estimates of longitudinal DIC export, air-water CO₂ fluxes, and mangrove-derived DIC inputs for the Shark and Harney Rivers. The results show that air-water CO₂ exchange and longitudinal DIC fluxes account for ca. 90% of the mangrove-derived dissolved carbon export out of the Shark and Harney Rivers, with the remainder being exported as dissolved organic carbon.

The mangrove contribution to the total longitudinal flux was 6.5 to 8.9% for DIC and 4 to 18% for DOC. A
605 lower bound estimate of the dissolved carbon export (DIC and DOC) from the forest surrounding Shark River during
the wet season was 18.9 to 24.5 mmol m⁻² d⁻¹ with 15.9 km² of mangrove contributing area. This basin-scale estimate
is somewhat lower by comparison than other independent estimates of lateral carbon export from this mangrove forest.
However, mangrove forest carbon export rates on an aerial basis are expected to vary with the spatial and temporal
610 scales over which they are calculated, and depend on factors such as tidal inundation frequency, distance from the
riverbank and the coast, and forest and soil characteristics.

Future experiments should investigate the contribution of DIC from groundwater to the rivers, by making
measurements of $\delta^{13}\text{C}_{\text{DIC}}$ of groundwater, Sr and Ca concentrations in the river to quantify CaCO₃ dissolution and to
separate carbonate alkalinity from TAlk, radon to quantify groundwater discharge, $^{14}\text{C}_{\text{DIC}}$ to separate input of DIC
from remineralization of organic matter from dissolution of CaCO₃. Experiments should also examine the seasonal
615 variability in the carbon dynamics and export, by conducting process-based studies like SharkTReX during both wet
and dry seasons. Also, time series measurement of current velocities, wind speeds, pCO₂ and pH (to calculate DIC),
DO, chromophoric dissolved organic matter (CDOM, as a proxy for DOC), and radon will also allow the temporal
variability of the sources and sinks of DIC in these rivers to be examined.

Author contribution

620 D. Ho, S. Ferron, and V. Engel conceived and executed the experiment, interpreted the data, and prepared the
manuscript with input from the other authors. W. Anderson measured the samples for $\delta^{13}\text{C}$ of dissolved organic carbon,
P. Swart measured the samples for $\delta^{13}\text{C}$ of dissolved inorganic carbon, R. Price measured the total alkalinity samples
for SharkTReX 1, and L. Barbero measured the total alkalinity and dissolved inorganic carbon samples for SharkTReX
2.

Data availability

625 The pCO₂ data collected during SharkTReX 1 and 2 are available from the SOCAT database <www.socat.info>. The
other data may be obtained by contacting the corresponding author.

Acknowledgments

We thank J. Barr, T. Custer, L. Larsen, M. Reid, and M. Vázquez-Rodríguez for assistance in the field, A. Arik, N.
630 Coffineau and J. Harlay for assistance with data analysis, R. Wanninkhof and R. Zeebe for helpful discussions and
comments, M. Sukop for the use of his laboratory, P. Sullivan for analyzing the total alkalinity samples during

SharkTREx 1. K. Kotun and Everglades National Park provided boats, fuel, and logistical support for the experiment. Shark River flow velocity data were obtained from USGS via the National Water Information System. Funding was provided by National Park Service through the Critical Ecosystem Studies Initiative (Cooperative Agreement H5284-08-0029) and by National Science Foundation through the Water Sustainability and Climate solicitation (EAR 1038855). R.M.P. was supported by the Florida Coastal Everglades Long-Term Ecological Research program under National Science Foundation Grant Nos. DBI-0620409 and DEB-1237517. This is SERC contribution number ####. Any use of trade, product, or firm names is for descriptive purposes only and does not imply endorsement by the U.S. Government.

640 **References**

- Alongi, D. M.: Coastal Ecosystem Processes, CRC Marine Science Series, edited by: Kennish, M. J., and Lutz, P. L., CRC press, Boca Raton, 448 pp., 1998.
- Alongi, D. M., Pfitzner, J., Trott, L. A., Tirendi, F., Dixon, P., and Klumpp, D. W.: Rapid sediment accumulation and microbial mineralization in forests of the mangrove *Kandelia candel* in the Jiulongjiang Estuary, China, *Estuar. Coast. Shelf Sci.*, 63, 605-618, 10.1016/j.eccs.2005.01.004, 2005.
- 645 Anderson, W. T., and Fourqurean, J. W.: Intra- and interannual variability in seagrass carbon and nitrogen stable isotopes from south Florida, a preliminary study, *Organic Geochemistry*, 34, 185-194, 10.1016/S0146-6380(02)00161-4, 2003.
- 650 Barr, J. G., Engel, V., Smith, T. J., and Fuentes, J. D.: Hurricane disturbance and recovery of energy balance, CO₂ fluxes and canopy structure in a mangrove forest of the Florida Everglades, *Agric. For. Meteorol.*, 153, 54-66, 10.1016/j.agrformet.2011.07.022, 2012.
- Barr, J. G., Fuentes, J. D., DeLonge, M. S., O'Halloran, T. L., Barr, D., and Ziemann, J. C.: Summertime influences of tidal energy advection on the surface energy balance in a mangrove forest, *Biogeosciences*, 10, 501-511, Doi 10.5194/Bg-10-501-2013, 2013.
- 655 Bergamaschi, B. A., Krabbenhoft, D. P., Aiken, G. R., Patino, E., Rumbold, D. G., and Orem, W. H.: Tidally Driven Export of Dissolved Organic Carbon, Total Mercury, and Methylmercury from a Mangrove-Dominated Estuary, *Environ. Sci. Technol.*, 46, 1371-1378, 10.1021/es2029137, 2011.
- Borges, A. V., Djenidi, S., Lacroix, G., Théate, J., Delille, B., and Frankignoulle, M.: Atmospheric CO₂ flux from mangrove surrounding waters, *Geophys. Res. Lett.*, 30, 1558, 10.1029/2003GL017143, 2003.
- 660 Borges, A. V.: Do we have enough pieces of the jigsaw to integrate CO₂ fluxes in the coastal ocean?, *Estuaries*, 28, 3-27, 10.1007/BF02732750, 2005.
- Bouillon, S., Frankignoulle, M., Dehairs, F., Velimirov, B., Eiler, A., Abril, G., Etcheber, H., and Borges, A. V.: Inorganic and organic carbon biogeochemistry in the Gautami Godavari estuary (Andhra Pradesh, India) during pre-monsoon: The local impacts of extensive mangrove forests, *Glob. Biogeochem. Cycle*, 17, 10.1029/2002GB002026, 2003.
- 665 Bouillon, S., Dehairs, F., Schiettecatte, L.-S., and Borges, A. V.: Biogeochemistry of the Tana estuary and delta (northern Kenya), *Limnol. Oceanogr.*, 52, 46-59, 10.4319/lo.2007.52.1.0046, 2007a.
- Bouillon, S., Dehairs, F., Velimirov, B., Abril, G., and Borges, A. V.: Dynamics of organic and inorganic carbon across contiguous mangrove and seagrass systems (Gazy Bay, Kenya), *J. Geophys. Res.*, 112, 10.1029/2006JG000325, 2007b.
- 670 Bouillon, S., Middelburg, J. J., Dehairs, F., Borges, A. V., Abril, G., Flindt, M. R., Ulomi, S., and Kristensen, E.: Importance of intertidal sediment processes and porewater exchange on the water column biogeochemistry in a pristine mangrove creek (Ras Dege, Tanzania), *Biogeosciences*, 4, 311-322, 10.5194/bg-4-311-2007, 2007c.
- Bouillon, S., Borges, A. V., Castañeda-Moya, E., Diele, K., Dittmar, T., Duke, N. C., Kristensen, E., Lee, S. Y., Marchand, C., Middelburg, J. J., Rivera-Monroy, V. H., Smith, T. J., and Twilley, R. R.: Mangrove production and carbon sinks: A revision of global budget estimates, *Glob. Biogeochem. Cycle*, 22, GB2013, 10.1029/2007GB003052, 2008a.
- Bouillon, S., Connolly, R. M., and Lee, S. Y.: Organic matter exchange and cycling in mangrove ecosystems: Recent insights from stable isotope studies, *Journal of Sea Research*, 59, 44-58, 10.1016/j.seares.2007.05.001, 2008b.
- 680 Boyer, J. N., Fourqurean, J. W., and Jones, R. D.: Spatial characterization of water quality in Florida Bay and Whitewater Bay by multivariate analyses: Zones of similar influence, *Estuaries*, 20, 743-758, 10.2307/1352248, 1997.
- Breithaupt, J. L., Smoak, J. M., Smith, T. J., and Sanders, C. J.: Temporal variability of carbon and nutrient burial, sediment accretion, and mass accumulation over the past century in a carbonate platform mangrove forest of the Florida Everglades, *J. Geophys. Res.*, 119, 2032-2048, 10.1002/2014JG002715, 2014.
- 685 Cai, W.-J., and Wang, Y.: The chemistry, fluxes, and sources of carbon dioxide in the estuarine waters of the Satilla and Altamaha Rivers, Georgia, *Limnol. Oceanogr.*, 43, 657-668, 1998.
- Call, M., Maher, D. T., Santos, I. R., Ruiz-Halpern, S., Mangion, P., Sanders, C. J., Erler, D. V., Oakes, J. M., Rosentreter, J., Murray, R., and Eyre, B. D.: Spatial and temporal variability of carbon dioxide and methane fluxes over semi-diurnal and spring-neap-spring timescales in a mangrove creek, *Geochim. Cosmochim. Acta*, 150, 211-225, 10.1016/j.gca.2014.11.023, 2015.
- 690 Castañeda-Moya, E., Twilley, R. R., Rivera-Monroy, V. H., Marx, B. D., Coronado-Molina, C., and Ewe, S. M. L.: Patterns of Root Dynamics in Mangrove Forests Along Environmental Gradients in the Florida Coastal Everglades, USA, *Ecosystems*, 14, 1178-1195, 10.1007/s10021-011-9473-3, 2011.

- 695 Castañeda-Moya, E., Twilley, R. R., and Rivera-Monroy, V. H.: Allocation of biomass and net primary productivity of mangrove forests along environmental gradients in the Florida Coastal Everglades, USA, *Forest Ecol Manag*, 307, 226-241, 10.1016/j.foreco.2013.07.011, 2013.
- Cawley, K. M., Yamashita, Y., Maie, N., and Jaffé, R.: Using Optical Properties to Quantify Fringe Mangrove Inputs to the Dissolved Organic Matter (DOM) Pool in a Subtropical Estuary, *Estuar Coast*, 37, 399-410, 10.1007/s12237-013-9681-5, 2013.
- 700 Chapin, F. S., Woodwell, G. M., Randerson, J. T., Rastetter, E. B., Lovett, G. M., Baldocchi, D. D., Clark, D. A., Harmon, M. E., Schimel, D. S., Valentini, R., Wirth, C., Aber, J. D., Cole, J. J., Goulden, M. L., Harden, J. W., Heimann, M., Howarth, R. W., Matson, P. A., McGuire, A. D., Melillo, J. M., Mooney, H. A., Neff, J. C., Houghton, R. A., Pace, M. L., Ryan, M. G., Running, S. W., Sala, O. E., Schlesinger, W. H., and Schulze, E.-D.: Reconciling Carbon-cycle Concepts, Terminology, and Methods, *Ecosystems*, 9, 1041-1050, 10.1007/s10021-005-0105-7, 2006.
- 705 DeNiro, M. J., and Epstein, S.: Influence of diet on the distribution of carbon isotopes in animals, *Geochim. Cosmochim. Acta*, 42, 495-506, 10.1016/0016-7037(78)90199-0, 1978.
- Dickson, A. G.: Standards for ocean measurements, *Oceanography*, 23, 34-47, 10.5670/oceanog.2010.22, 2010.
- Dittmar, T., and Lara, R. J.: Do mangroves rather than rivers provide nutrients to coastal environments south of the Amazon River? Evidence from long-term flux measurements, *Marine Ecology Progress Series*, 213, 67-77, 2001.
- 710 Dittmar, T., Hertkorn, N., Kattner, G., and Lara, R. J.: Mangroves, a major source of dissolved organic carbon to the oceans, *Glob. Biogeochem. Cycle*, 20, GB1012, 10.1029/2005GB002570, 2006.
- Fischer, H. B., List, E. J., Imberger, J., Koh, R. C. Y., and Brooks, N. H.: *Mixing in inland and coastal waters*, Academic Press, New York, 483 pp., 1979.
- Garcia, H. E., and Gordon, L. I.: Oxygen solubility in seawater: better fitting equations, *Limnol. Oceanogr.*, 37, 1307-1312, 10.4319/lo.1992.37.6.1307, 1992.
- 715 He, D., Mead, R. N., Belicka, L., Pisani, O., and Jaffé, R.: Assessing source contributions to particulate organic matter in a subtropical estuary: A biomarker approach, *Organic Geochemistry*, 75, 129-139, 10.1016/j.orggeochem.2014.06.012, 2014.
- Ho, D. T., Schlosser, P., and Caplow, T.: Determination of longitudinal dispersion coefficient and net advection in the tidal Hudson River with a large-scale, high resolution SF₆ tracer release experiment, *Environ. Sci. Technol.*, 36, 3234-3241, 10.1021/es015814+, 2002.
- Ho, D. T., Ferrón, S., Engel, V. C., Larsen, L. G., and Barr, J. G.: Air-water gas exchange and CO₂ flux in a mangrove-dominated estuary, *Geophys. Res. Lett.*, 41, 108-113, 10.1002/2013GL058785, 2014.
- 720 Ho, D. T., Coffineau, N., Hickman, B., Chow, N., Koffman, T., and Schlosser, P.: Influence of current velocity and wind speed on air-water gas exchange in a mangrove estuary, *Geophys. Res. Lett.*, 43, 10.1002/2016GL068727, 2016.
- 725 Howard, P. J. A.: The Carbon-Organic Matter Factor in Various Soil Types, *Oikos*, 15, 229-236, 10.2307/3565121, 1965.
- Jaffé, R., Mead, R., Hernandez, M. E., Peralba, M. C., and DiGuida, O. A.: Origin and transport of sedimentary organic matter in two subtropical estuaries: a comparative, biomarker-based study, *Org. Geoch.*, 32, 507-523, 10.1016/S0146-6380(00)00192-3, 2001.
- 730 Jähne, B., Munnich, K. O., Bosinger, R., Dutzi, A., Huber, W., and Libner, P.: On the parameters influencing air-water gas exchange, *J. Geophys. Res.*, 92, 1937-1949, 10.1029/JC092iC02p01937, 1987.
- Jennerjahn, T. C., and Ittekkot, V.: Relevance of mangroves for the production and deposition of organic matter along tropical continental margins, *Naturwissenschaften*, 89, 23-30, 10.1007/s00114-001-0283-x, 2002.
- 735 Keeling, R. F., and Manning, A. C.: Studies of Recent Changes in Atmospheric O₂ Content, in: *Treatise on Geochemistry (Second Edition)*, Second ed., edited by: Holland, H. D., and Turekian, K. K., Elsevier, Oxford, 385-404, 2014.
- Kieckbusch, D. K., Koch, M. S., Serafy, J. E., and Anderson, W. T.: Trophic linkages of primary producers and consumers in fringing mangroves of tropical lagoons, *Bulletin of Marine Science*, 74, 271-285, 2004.
- 740 Koné, Y. J.-M., and Borges, A. V.: Dissolved inorganic carbon dynamics in the waters surrounding forested mangroves of the Ca Mau Province (Vietnam), *Estuar. Coast. Shelf Sci.*, 77, 409-421, 10.1016/J.Ecss.2007.10.001, 2008.
- Kristensen, E., Bouillon, S., Dittmar, T., and Marchand, C.: Organic carbon dynamics in mangrove ecosystems: A review, *Aquatic Botany*, 89, 201-219, 10.1016/j.aquabot.2007.12.005, 2008.
- 745 Levesque, V. A.: Water Flow and Nutrient Flux from Five Estuarine Rivers along the Southwest Coast of the Everglades National Park, Florida, 1997-2001: U.S. Geological Survey Scientific Investigations Report 2004-5142, U.S. Geological Survey Scientific Investigations Report 2004-5142, 24, 2004.

Maher, D. T., Santos, I. R., Golsby-Smith, L., Gleeson, J., and Eyre, B. D.: Groundwater-derived dissolved inorganic and organic carbon exports from a mangrove tidal creek: The missing mangrove carbon sink?, *Limnol. Oceanogr.*, 58, 475-488, 10.4319/lo.2013.58.2.0475, 2013.

750 Mancera-Pineda, J. E., Twilley, R. R., and Rivera-Monroy, V. H.: Carbon ($\delta^{13}\text{C}$) and nitrogen ($\delta^{15}\text{N}$) isotopic discrimination in mangroves in Florida Coastal Everglades as a function of environmental stress, *Contributions in Marine Science*, 38, 109-129, 2009.

755 Miyajima, T., Tsuboi, Y., Tanaka, Y., and Koike, I.: Export of inorganic carbon from two Southeast Asian mangrove forests to adjacent estuaries as estimated by the stable isotope composition of dissolved inorganic carbon, *J. Geophys. Res.*, 114, G01024, 10.1029/2008JG000861, 2009.

Mook, W. G., and Tan, T. C.: Stable carbon isotopes in rivers and estuaries, in: *Biogeochemistry of the major world rivers*, SCOPE Report 42, edited by: Degens, E. T., Kempe, S., and Richey, J. E., John Wiley & Sons, Chichester, 245-264, 1991.

760 Pierrot, D., Lewis, E., and Wallace, D. W. R.: MS Excel Program Developed for CO₂ System Calculations. ORNL/CDIAC-105a. Carbon Dioxide Information Analysis Center, Oak Ridge National Laboratory, U.S. Department of Energy, Oak Ridge, Tennessee, 10.3334/CDIAC/otg.CO2SYS_XLS_CDIAC105a, 2006.

Price, R. M., Swart, P. K., and Fourqurean, J. W.: Coastal groundwater discharge – an additional source of phosphorus for the oligotrophic wetlands of the Everglades, *Hydrobiologia*, 569, 23-36, 10.1007/s10750-006-0120-5, 2006.

765 Rivera-Monroy, V. H., Twilley, R. R., Davis III, S. E., Childers, D. L., Simard, M., Chambers, R., Jaffé, R., Boyer, J. N., Rudnick, D. T., Zhang, K., Castañeda-Moya, E., Ewe, S. M. L., Price, R. M., Coronado-Molina, C., Ross, M., Smith III, T. J., Michot, B., Meselhe, E., Nuttle, W., Troxler, T. G., and Noe, G. B.: The role of the Everglades mangrove ecotone region (EMER) in regulating nutrient cycling and wetland productivity in South Florida, *Critical Reviews in Environmental Science and Technology*, 41, 663-669, 10.1080/10643389.2010.530907, 2011.

770 Rutherford, J. C.: River mixing, John Wiley & Sons, New York, 347 pp., 1994.

Saha, A., Moses, C., Price, R., Engel, V., Smith, T., III, and Anderson, G.: A Hydrological Budget (2002–2008) for a Large Subtropical Wetland Ecosystem Indicates Marine Groundwater Discharge Accompanies Diminished Freshwater Flow, *Estuar Coast*, 35, 459-474, 10.1007/s12237-011-9454-y, 2012.

775 Salomons, W., and Mook, W. G.: Isotope Geochemistry of Carbonates in the Weathering Zone, in: *Handbook of Environmental Isotope Geochemistry*, Vol 2, The Terrestrial Environment, B, edited by: Fritz, P., and Fontes, J. C., Elsevier, Amsterdam, 239-269, 1986.

Severinghaus, J. P.: Studies of the terrestrial O₂ and carbon cycle in sand dune gases and in Biosphere 2, Ph.D. thesis, Columbia University, New York, 50 pp., 1995.

780 Troxler, T. G., Barr, J. G., Fuentes, J. D., Engel, V., Anderson, G., Sanchez, C., Lagomasino, D., Price, R., and Davis, S. E.: Component-specific dynamics of riverine mangrove CO₂ efflux in the Florida coastal Everglades, *Agric. For. Meteorol.*, 213, 273-282, 10.1016/j.agrformet.2014.12.012, 2015.

Twilley, R. R., Chen, R. H., and Hargis, T.: Carbon sinks in mangroves and their implications to carbon budget of tropical coastal ecosystems, *Water, Air and Soil Pollution*, 64, 265-288, 10.1007/BF00477106, 1992.

785 U.S. Geological Survey: National Water Information System data available on the World Wide Web (USGS Water Data for the Nation), accessed February 10, 2016, at url <http://waterdata.usgs.gov/nwis/>. 2016.

Wanninkhof, R.: Relationship between wind speed and gas exchange over the ocean revisited, *Limnol. Oceanogr. Methods*, 12, 351-362, 10.4319/lom.2014.12.351, 2014.

790 Weiss, R. F.: Carbon dioxide in water and seawater: the solubility of a non-ideal gas, *Mar. Chem.*, 2, 203-215, 10.1016/0304-4203(74)90015-2, 1974.

Ya, C., Anderson, W., and Jaffé, R.: Assessing dissolved organic matter dynamics and source strengths in a subtropical estuary: Application of stable carbon isotopes and optical properties, *Continental Shelf Research*, 92, 98-107, 10.1016/j.csr.2014.10.005, 2015.

Zhang, J., Quay, P. D., and Wilbur, D. O.: Carbon isotope fractionation during gas-water exchange and dissolution of CO₂, *Geochim. Cosmochim. Acta*, 59, 107-114, 10.1016/0016-7037(95)91550-D, 1995.

795

Table 1. Inventories of DIC and DOC in Shark and Harney Rivers, as well as contributions from estuarine and non-estuarine sources.

	SharkTREx 1					SharkTREx 2						
	Shark River		Shark River			Shark River		Harney River				
	Inventory ^a (x10 ⁶ mol)	Percentage of total Inventory ^b	Proportion of mangrove carbon ^ε	Proportion of total carbon ^d	Inventory ^a (x10 ⁶ mol)	Percentage of total Inventory ^b	Proportion of mangrove carbon ^ε	Proportion of total carbon ^d	Inventory ^a (x10 ⁶ mol)	Percentage of total Inventory ^b	Proportion of mangrove carbon ^ε	Proportion of total carbon ^d
DIC	Observed	19.5 ± 0.9	-			15.2 ± 1.3	-		7.4 ± 0.4	-		
	Gas Exchange	2.5 ± 0.2	11%			3.2 ± 0.1	17%		1.5 ± 0.3	17%		
	Non-estuarine	17.6 ± 0.7	80%	94%	82%	13.6 ± 1.2	74%	93%	6.5 ± 0.4	72%	93%	79%
	Estuarine	4.4 ± 1.1	20%			4.8 ± 1.8	26%		2.5 ± 0.6	28%		
	Mangrove	2.9 ± 0.8	13%			3.1 ± 1.2	17%		1.7 ± 0.4	19%		
DOC	Observed	4.4 ± 0.1				4.1 ± 0.4			1.9 ± 0.1			
	Non-estuarine	4.2 ± 0.1	96%	6%	18%	3.9 ± 0.4	94%	7%	1.8 ± 0.1	93%	7%	21%
	Estuarine ^c	0.2 ± 0.1	4%			0.2 ± 0.6	6%		0.1 ± 0.2	7%		

^a The uncertainty in the observed and non-estuarine inventories are the standard deviations of the inventories for all the days of the experiment. The estuarine contribution is calculated from the observed and non-estuarine contribution, and the uncertainty is from propagating the errors of the two. The uncertainty in contribution from gas exchange is from propagating the uncertainty in CO₂ flux and the residence time. The uncertainty in mangrove contribution is calculated from propagating the error from the estuarine contribution.

^b The DIC inventory is relative to the total DIC (i.e., $\sum[\text{DIC}]_{\text{observed}} + \sum[\text{DIC}]_{\text{gasex}}$).

Deleted: Contribution to

Deleted: ^c

Deleted: ^c

Deleted: ^c

Deleted: ^a

Deleted: ^a

Deleted: ^a

Deleted: ^b

Deleted: ^b

Deleted: ^b

Deleted: Estuarine^d

Deleted: ^a

800

820

^c [Proportion](#) of each form of carbon (i.e., DIC, DOC) [relative](#) to the total mangrove-derived carbon pool.

^d [Proportion](#) of each form of carbon (i.e., DIC, DOC) [relative](#) to the total carbon pool.

^e Estuarine DOC is assumed to be entirely of mangrove origin.

Deleted: ^b Contribution

Deleted: ^c Contribution

Deleted: ^d

Table 2. Longitudinal DIC and DOC fluxes, and air-water CO₂ fluxes for the Shark and Harney Rivers during SharkTREx 1 and 2.

	SharkTREx 1		SharkTREx 2	
	Shark River	Harney River	Shark River	Harney River
<i>Longitudinal DIC Fluxes ($\times 10^5 \text{ mol d}^{-1}$)^a</i>				
Total	33.6 ± 1.6	N/A	18.8 ± 1.6	15.8 ± 0.9
Non-estuarine contribution	30.3 ± 1.1	N/A	16.8 ± 1.5	13.7 ± 0.8
Estuarine Contribution	3.3 ± 1.9	N/A	2.0 ± 2.2	2.1 ± 1.3
Mangrove Contribution	2.2 ± 1.3	N/A	1.3 ± 1.5	1.4 ± 0.8
<i>Air-Water CO₂ Fluxes ($\times 10^5 \text{ mol d}^{-1}$)^a</i>				
Total	4.2 ± 0.4	4.1 ± 0.2	4.0 ± 0.2	3.1 ± 0.6
Non-estuarine contribution	2.1 ± 0.2	2.0 ± 0.1	1.9 ± 0.1	1.1 ± 0.2
Estuarine Contribution	2.1 ± 0.4	2.1 ± 0.3	2.1 ± 0.2	2.0 ± 0.6
Mangrove Contribution	1.4 ± 0.3	1.4 ± 0.2	1.4 ± 0.1	1.3 ± 0.4
<i>Longitudinal DOC Fluxes ($\times 10^5 \text{ mol d}^{-1}$)^{a,b}</i>				
Total	7.5 ± 0.2	3.3 ± 0.4	5.1 ± 0.5	4.2 ± 0.2
Non-estuarine contribution	7.2 ± 0.1	2.6 ± 0.3	4.8 ± 0.5	3.9 ± 0.2
Estuarine Contribution ^c	0.3 ± 0.2	0.6 ± 0.6	0.3 ± 0.7	0.3 ± 0.3

Deleted: ^b

830

^a Uncertainty in total and non-estuarine fluxes are from propagating the error in total inventory and the residence time. The uncertainty in the estuarine fluxes are from propagating the errors in total and non-estuarine fluxes. The uncertainty in mangrove contribution is from propagating the errors in the estuarine contribution.

Deleted: ^a

^b Data for DOC concentration in Harney River during SharkTREx 1 taken from *Cawley et al. (2013)*.

^c Estuarine contribution to DOC is assumed to be entirely of mangrove origin.

Deleted: ^b

Table 3. Mangrove contribution to $\Sigma[\text{DIC}]_{\text{estuary}}$ determined from $\delta^{13}\text{C}_{\text{DIC}}$ mass balance and TAlk/DIC ratios.

River	Experiment	Methods	
		$\delta^{13}\text{C}_{\text{DIC}}$	TAlk/DIC
Shark River	SharkTREx 1	60 ± 6%	70 ± 3%
	SharkTREx 2	61 ± 6%	70 ± 3%
Harney River	SharkTREx 1	-	-
	SharkTREx 2	61 ± 6%	70 ± 2%

840

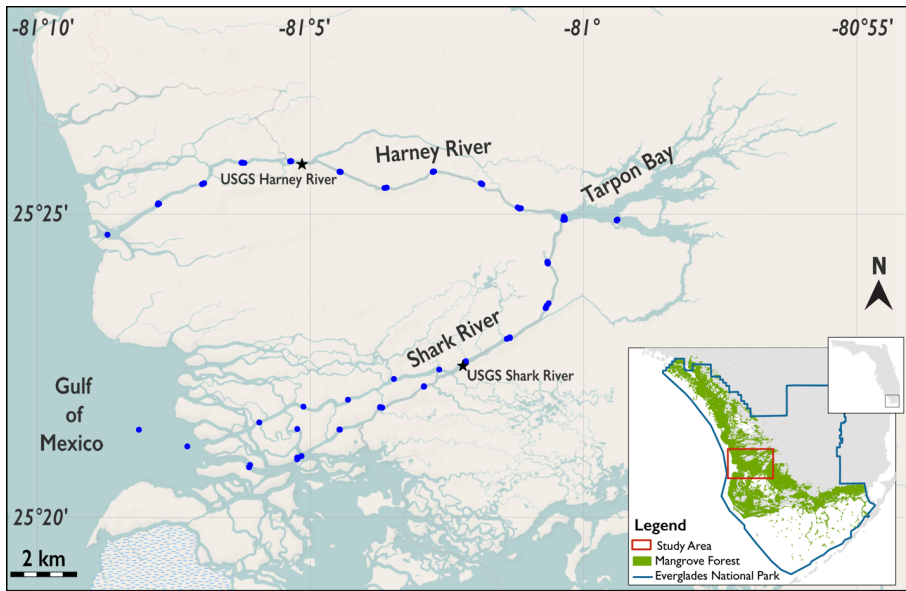
Table 4. Distribution of total and mangrove fluxes of DIC and DOC for Shark and Harney Rivers during SharkTREx 1 and 2.

		SharkTREx Experiment #	Estuarine Contribution ^a	Percent of Total Export Flux ^b	Percent of total Mangroves Flux ^c
Longitudinal DIC Flux	Shark River	1	10%	74%	57%
		2	11%	67%	45%
	Harney River	1	-	-	-
		2	13%	68%	48%
Air-Water CO ₂ Flux	Shark River	1	49%	9%	35%
		2	52%	14%	45%
	Harney River	1	51%	-	-
		2	63%	14%	43%
All DIC Fluxes	Shark River	1		83%	92%
		2		82%	90%
	Harney River	1		-	-
		2		82%	91%
Longitudinal DOC Flux	Shark River	1	4%	17%	8%
		2	6%	18%	10%
	Harney River	1	19%	-	-
		2	7%	18%	9%

^a Estuarine contribution to the individual fluxes in each river during each experiment

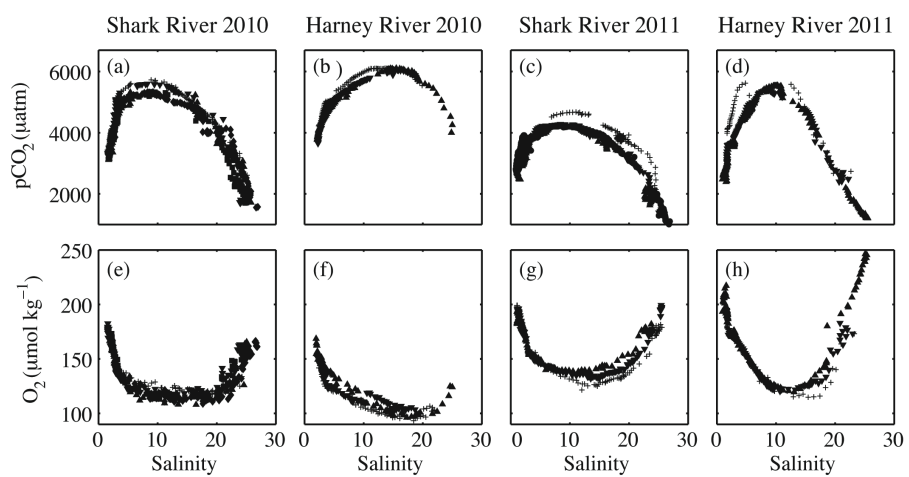
845 ^b Flux as a percentage of the total dissolved carbon flux (i.e., longitudinal DIC, DOC and air-water CO₂ fluxes)

^c Flux as a percentage of the total mangrove-derived dissolved carbon flux (i.e., longitudinal DIC, DOC and air-water CO₂ fluxes)



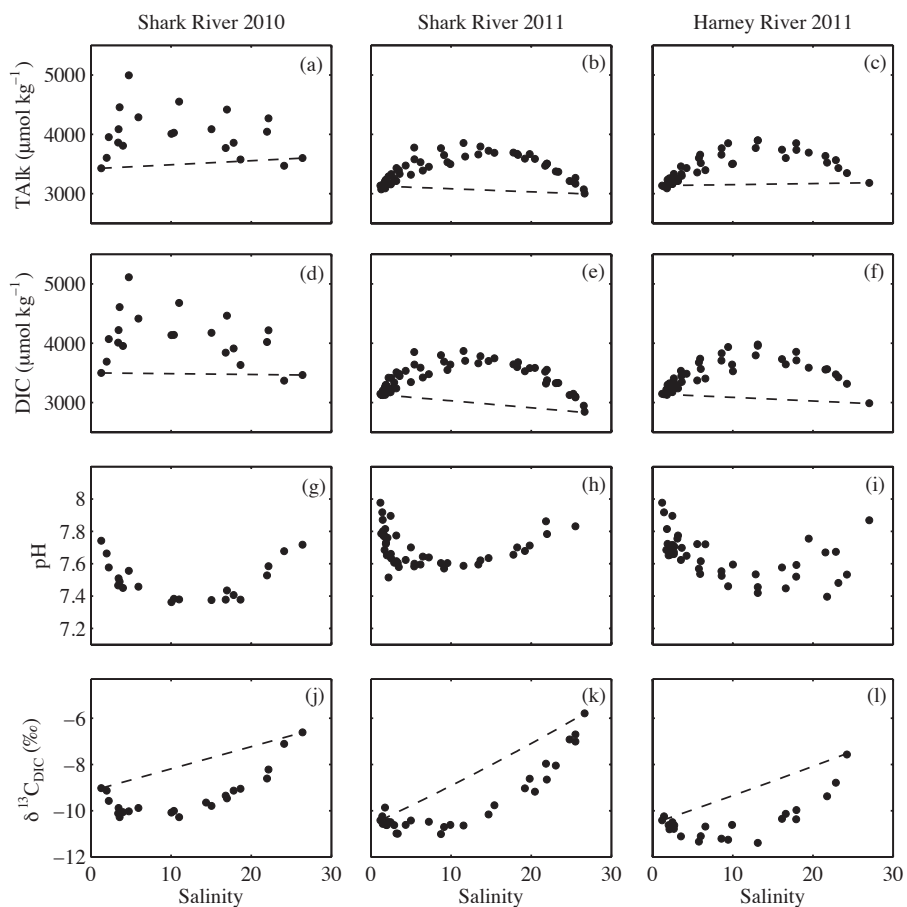
850

Figure 1. Map of the study area near the southern tip of Florida, USA, showing locations of Shark River, Harney River, and Tarpon Bay. The blue circles indicate the locations where discrete samples were taken, and the black stars denote the USGS gaging stations on both rivers. The green areas in the inset are part of the largest contiguous mangrove forest in North America. Indicated in the inset are the boundaries of Everglades National Park.



855

Figure 2. Distributions of $p\text{CO}_2$ (a-d) and dissolved O_2 (e-h) along the salinity gradient in the Shark and Harney Rivers during the 2010 (SharkTREx 1) and 2011 (SharkTREx 2) campaigns. Different symbols represent measurements made on different days.



860

Figure 3. Distribution of TALK (a-c), DIC (d-f), pH (g-i) and $\delta^{13}\text{C}_{\text{DIC}}$ (j-l) along the salinity gradient in the Shark and Harney Rivers during the 2010 (SharkTREx 1) and 2011(SharkTREx 2) campaigns. During SharkTREx 1, TALK and pH were measured at FIU, and DIC was calculated using CO2SYS (Pierrot et al., 2006). During SharkTREx 2, DIC and TALK were measured at NOAA/AOML, and pH was calculated using CO2SYS. The dashed lines indicate the distribution expected for conservative mixing.

865

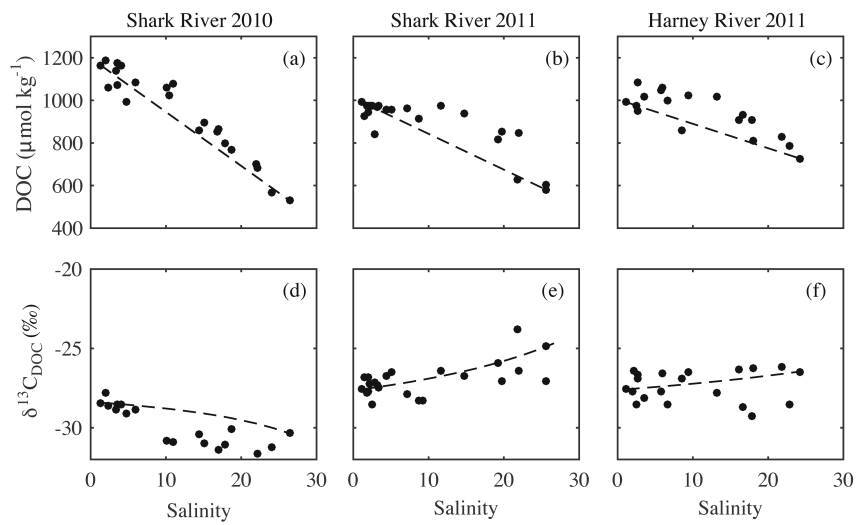


Figure 4. Distribution of DOC and $\delta^{13}\text{C}_{\text{DOC}}$ along the salinity gradient in the Shark and Harney Rivers in samples collected during SharkTREx 1 and 2. The dashed lines indicate the distribution expected for conservative mixing.

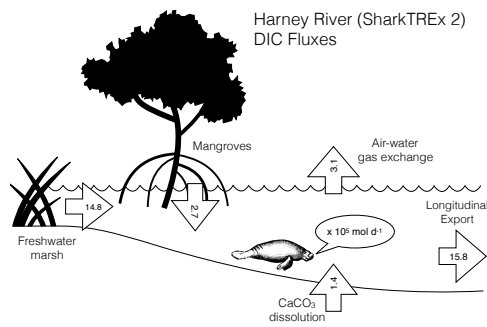
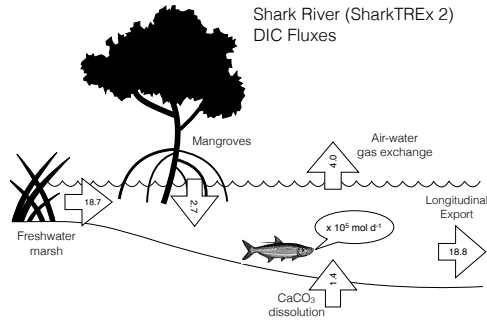
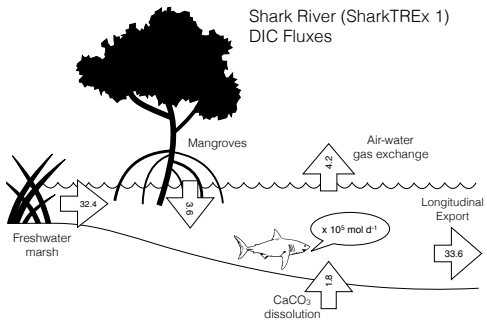


Figure 5. Diagrams showing the main DIC fluxes (in 10^5 mol d^{-1}) entering and exiting the Shark and Harney Rivers during SharkTREx 1 and 2. Fluxes from the freshwater marsh were assumed to be fluxes estimated from the conservative DIC curves.

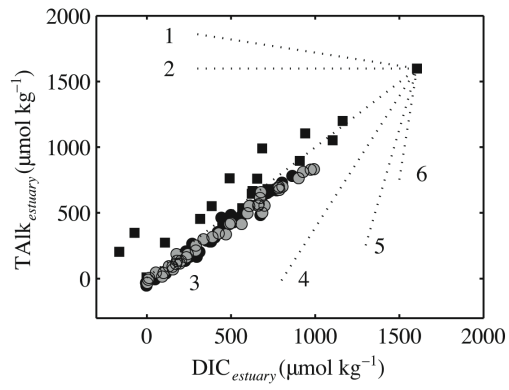


Figure 6. (a) Covariation of $\text{DIC}_{\text{estuary}}$ and $\text{TAlk}_{\text{estuary}}$. Black squares are samples from the Shark River during SharkTREX 1, and black and gray circles are from the Shark and Harney Rivers, respectively, during SharkTREX 2. Dotted lines represent the theoretical covariation of DIC and TAlk for different biogeochemical processes: 1) aerobic respiration; 2) CO_2 emission, 3) sulfate reduction, 4) CaCO_3 dissolution, 5) manganese reduction, and 6) iron reduction.